Editorial Board

Climate of the Past

Dear Prof. Alberto Reyes

Reply to reviewer comments on MS No.: cp-2019-138

We thank you for your time and effort in reviewing our manuscript "Aridification signatures from fossil pollen indicate a drying climate in east-central Tibet during the late Eocene". Below we provide responses to the comments with line numbers indicating where we have made changes, and include a separate marked-up manuscript version showing the changes made.

Please be advised, line numbers below refer to lines in the marked-up version of the document, not the clean copy.

Comments to the Author

1. Yuan et al 2017 Paleoworld paper gives a slightly different account of the stratigraphic framework for the Gongjue Fm: the 2017 paper describes three members for the formation as a whole, but this manuscript gives those same three members within only the Eg3 unit of the formation. Please clarify for readers.

Thank you for pointing this out. We realised that the stratigraphy described in Yuan et al. (2017, Paleoworld) was incorrect when checking the original papers in Chinese of Wang and Wang (2001, 2002) and Du et al. (2011). We have now made this clear for readers in Lines 162-165.

2. I realize that authors are preparing a separate manuscript with details on lithostrat, geochemistry, etc for this section. But because there is no published information on this section it is fair to ask for at least some additional brief details. Something like Table 1 in the Yuan et al 2017 paper would be sufficient, along with some representative photographs similar to Fig 2 of that same paper. Are there any potential linkages between lithofacies in the upper part of the section and the poor sample productivity in Zones 2 and 3? If so, please add some short on this point, since the poor pollen recovery in those zones is certainly problematic (as the authors already point out).

We now added a new figure (Fig. 2) illustrating the lithologies of the Ria Zhong (RZ) section. Field photographs of the section with palynological zones marked, and images of the representative lithologies are included. A new table (Table 1) has also been added, giving further details on the lithostratigraphy of the RZ section (Lines 191-202).

We added a discussion on the linkage between lithofacies in the upper part of the section and the poor sample productivity in Zones 2 and 3 in Lines 230-235.

3. Somewhat related to the point above, I think it's fair to ask that authors be even more circumspect about the problematic low pollen recovery from sediments assigned to Zones 2 and 3. This could be done easily at the start of the Results (lines 214): "Recovery is particularly poor in the upper half (~xx m) of the section." This should then be followed up with caveats in the results section for those zones (section 4.1.2 and 4.1.3).

We have now added these points in Lines 230, 332-334, and 340-341.

4. Authors have noted at one point in the Discussion that the tropical forest "spike" is only present in one sample, but elsewhere in the Discussion (lines 372 and 374) this spike is assigned to the entire Zone 2. Please revise to make it crystal clear that this spike only applies to one sample. e.g ".....a significant spike in tropical forest pollen in one sample..." and "Although the increase in tropical forest taxa in one sample from this zone does not indicate..."

We now added this text in Lines 244, 329, 401 and 403.

5. Very minor point: on line 200 you say you followed the approach of Hoorn et al to assign taxa to PFTs. Can you clarify if you followed the taxon-to-NLR assignments provided by Hoorn? If there are any deviations from this, or if this is not what you meant, please provide a supplemental table that explicitly gives the NLR and PFT associated with each taxon. Hmm, on second thought the supplemental pollen diagrams probably accomplish this already for the PFTs, at least.

Yes, we followed the taxon-to-NLR assignments of Hoorn et al. (2012) without deviations. PFTs are shown in the supplementary dataset of Yuan & Barbolini (2020) for which the DOI is provided in the paper, as well as Fig. S1 and S2. We now added this text for readers in Lines 215-217 so they can easily find the information should they wish to.

Aridification signatures from fossil pollen indicate a drying climate in east-central Tibet during the late Eocene

Qin Yuan[a,b,c,d*], Natasha Barbolini[e,f], Catarina Rydin[e,g], Dong-Lin Gao[a,b], Hai-Cheng Wei[a,b], Qi-Shun Fan[a,b], Zhan-Jie Qin[a,b], Yong-Sheng Du[a,b], Jun-Jie Shan[a,b,c], Fa-Shou Shan[a,b], Vivi Vajda[d]

[a] *Key Laboratory of Comprehensive and Highly Efficient Utilization of Salt Lake Resources, Qinghai Institute of Salt Lakes, Chinese Academy of Sciences, Xining, China*

[b] *Qinghai Provincial Key Laboratory of Geology and Environment of Salt Lakes, Qinghai Institute of Salt Lakes, Chinese Academy of Sciences, Xining, China*

[c] *University of Chinese Academy of Sciences, Beijing 100049, China*

[d] *Department of Palaeobiology, Swedish Museum of Natural History, Stockholm, Sweden*

[e] *Department of Ecology, Environment and Plant Sciences and Bolin Centre for Climate Research, Stockholm University, SE-106 91 Stockholm, Sweden*

[f] *Department of Ecosystem and Landscape Dynamics, Institute for Biodiversity and Ecosystem Dynamics, University of Amsterdam, 1098 XH The Netherlands*

[g] *The Bergius Foundation, The Royal Swedish Academy of Sciences, Box 50005, SE-104 05 Stockholm, Sweden*

Correspondence to: Natasha Barbolini (barbolini.natasha@gmail.com)

Abstract. Central Asia experienced a number of significant elevational and climatic changes during the Cenozoic, but much remains to be understood regarding the timing and driving mechanisms of these changes, as well as their influence on ancient ecosystems. Here we describe the palaeoecology and palaeoclimate of a new section from the Nangqian Basin in Tibet, northwestern China, here dated as Bartonian (41.2–37.8 Ma; late Eocene) based on our palynological analyses. Located on the east-central part of what is today the Tibetan Plateau, this section is excellently placed for better understanding the palaeoecological history of Tibet following the India-Asia collision. Our new palynological record reveals that a strongly seasonal steppe-desert ecosystem characterised by drought-tolerant shrubs, diverse ferns and an underlying component of broad-leaved forests existed in east-central Tibet during the Eocene, influenced by a southern monsoon. A transient warming event, possibly the Middle Eocene Climatic Optimum (MECO; 40 Ma), is reflected in our record by a temporary increase in regional tropical taxa and a concurrent decrease in steppe-desert vegetation. In the late Eocene, a

drying signature in the palynological record is linked to proto-Paratethys sea retreat, which caused widespread

long-term aridification across the region. To better distinguish between local climatic variation and farther-

reaching drivers of Central Asian palaeoclimate and elevation, we correlated key palynological sections across

the Tibetan Plateau by means of established radioisotopic ages and biostratigraphy. This new palynozonation

illustrates both intra- and inter-basinal floral response to Qinghai-Tibetan uplift and global climate change

during the Paleogene, and provides a framework for the age assignment of future palynological studies in

Central Asia. Our work highlights the ongoing challenge of integrating various deep time records for the

purpose of reconstructing palaeoelevation, indicating that a multiproxy approach is vital for unravelling the

complex uplift history of Tibet and its resulting influence on Asian climate.

1. Introduction

A series of major geological events occurred during the Cenozoic, which led to a fundamental change in

the global climate (Zachos et al., 2001). The most important events include the formation of the polar ice cap

(e.g., DeConto and Pollard, 2003; Pagani et al., 2011), regression of the proto-Paratethys Sea from Eurasia

(Abels et al., 2011; Bosboom et al., 2014; Caves et al., 2015; Bougeois et al., 2018; Kaya et al., 2019; Meijer et

al., 2019), and uplift of the Qinghai-Tibetan region (Dupont-Nivet et al., 2007, 2008; Molnar et al., 2010; Miao

et al., 2012; Hu et al., 2016; Li et al., 2018). Today the Tibetan Plateau (TP) is the highest elevated plateau in the

world, with a complex uplift history beyond a simple collision between the Indian and Asian continents (Molnar

and Tapponnier, 1975; Aitchison and Davis, 2001; Wang, C.S., et al., 2008; Xia et al., 2011; Aitchison et al.,

2011; Zhang et al., 2012; Wang, C.W., 2014; Spicer et al., 2020). Here, the term 'Tibetan Plateau' is used in the

paper to denote the geographic extent occupied by the modern plateau, but should not be taken to imply that an

elevated expanse of low relief topography existed across this region in the Eocene (Spicer et al., 2020).

Previous studies indicate that retreat of the proto-Paratethys Sea and the uplift of Tibet as well as other

ranges to the north, such as the Altai, Sayan, and Hangay (Caves et al., 2014), may have been responsible for

monsoon intensification and aridification across the Asian continental interior in the Paleogene, although the

timing of these mechanisms, and their roles in forcing climate dynamics, are still debated (Caves et al., 2015;

Spicer, 2017). In particular, a lack of consensus exists regarding the onset of Asian aridification, whether it was

a Paleogene or Neogene phenomenon, and its relationship with Tibetan uplift (e.g., Dupont-Nivet et al. 2007;

Xiao et al., 2010; Miao et al., 2012; Caves et al., 2015; Liu et al., 2016; Wang et al., 2018; Li L. et al., 2019;

58 Paeth et al., 2019). Aridification in northeastern Tibet appears to have intensified after the Middle Eocene

59 Climatic Optimum (MECO;~ 40 Ma), a short-lived warming event documented in marine records globally. The

60 drying climate after this event is primarily linked to the second regression of the proto-Paratethys Sea, which

61 reduced moisture supply via the westerlies to Central Asia (Kaya et al., 2019). In northeastern Tibet, the regional

62 disappearance of perennial lakes, accompanied by an increase in pollen from xerophytic plants, marks a

63 permanent aridification step in the Asian terrestrial record after ~40 Ma (Bosboom et al., 2014); however, these

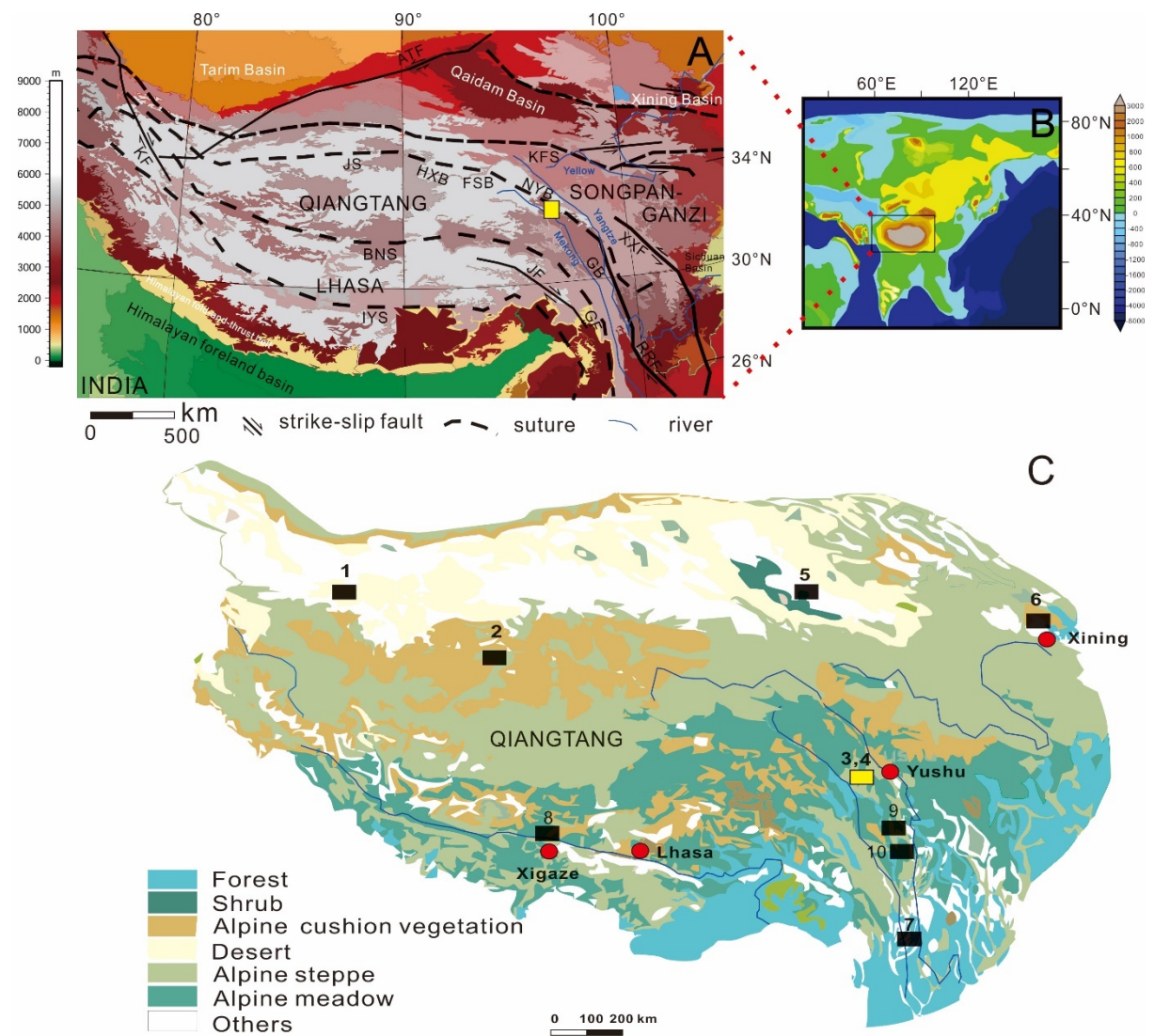64 climatic trends are yet to be identified in central Tibet.

65

67 **Figure 1: (A) Tectonic map of the Tibetan Plateau (TP) with major sedimentary basins (HXB: Hoh Xil Basin; FSB:**

68 **Fenghuo Shan basins; NYB: Nangqian-Yushu basins; GB: Gongjo Basin), sutures (JS: Jinsha suture; BNS: Bangong-**

69 **Nujiang suture; IYS: Indus-Yalu suture), and major faults (KF: Karakorum fault; ATF: Altyn Tagh fault; KFS:**

70 **Kunlun fault system; XXF: Xiangshuihe-Xiaojiang fault system; RRF: Red River fault; GF: Gaoligong fault; JF:**

71 **Jiali fault) indicated, redrawn after Horton et al. (2002). The yellow rectangle indicates the location of this study in**

3

The uplifting, large-scale thrusting and striking of Tibet caused several Paleogene intracontinental basins to form within the northern and central Qinghai-Tibetan region, including the Nangqian Basin. Situated in the Yushu area (Fig. 1), this basin lies directly above the Lhasa terrane, which comprised part of NE Gondwana in the Late Triassic to Early Jurassic and formed through a subduction–accretion process similar to that of the later India–Asia collision (Liu et al., 2009). Subsequent to its formation, the Nangqian Basin was infilled with non-marine sedimentary deposits (Wang et al., 2001; 2002), and is now a key site for understanding the Cenozoic tectonics, palaeoelevation and paleoclimatic changes that took place in the Qinghai-Tibetan region since the collision of the Indian and Asian tectonic plates (Gupta et al., 2004; Molnar, et al., 2004; Wang et al., 2001). Previous palynological studies from this part of the plateau revealed a relatively dry climate with brief humid intervals in the late Eocene, dominated by drought-tolerant (xerophytic) and salt-tolerant (halophytic) steppe-desert vegetation (Wei, 1985; Yuan et al., 2017).

This climate and palaeoflora were very similar to contemporaneous plateau ecosystems further to the north, such as the Xining (Dupont-Nivet et al. 2007, 2008; Hoorn et al., 2012) and Hoh Xil (Liu et al., 2003; Miao et al., 2016) basins, demonstrating the potential for these successions to be biostratigraphically correlated. Furthermore, oxygen isotope records indicate that both northern and east-central Tibet received moisture dominantly via the westerlies, which have maintained a semi-arid to arid climate in Central Asia since the early Eocene (Caves et al., 2015; Caves Rugenstein and Chamberlain, 2018. This suggests that aridification across this part of Tibet in the Eocene was related to large-scale atmospheric transport, and justifies a comparison of palynological records in the northern and central parts of the TP.

In contrast, southeastern Tibet seems to have experienced a more humid climate hosting widespread conifer and warm-temperate broad-leaved forests (Li et al., 2008; Su et al., 2018), likely influenced by a Paleogene Inter-tropical Convergence Zone (ITCZ) -driven monsoon system similar to the modern Indonesia-Australia Monsoon (I-AM; Spicer et al., 2017). Today this summer-wet, winter-dry monsoonal regime presides over a biodiversity hotspot in southern Asia; similarly seasonal climates in the past are thought to also have

103   stimulated high biodiversity (Spicer, 2017). Southerly moisture has probably rarely extended northward of the

104   central TP (Caves Rugenstein and Chamberlain, 2018); moreover, southern Tibetan Eocene floras display a

105   modern aspect (e.g., Linnemann et al., 2018) that is quite different to more ancestral steppe vegetation hosted in

106   the northern TP.

107   The extent and timing of mechanisms that promoted somewhat different floras south and north of the

108   Tibetan–Himalayan orogen remain poorly understood, with Licht et al. (2014) reporting marked monsoon-like

109   patterns in both regions during the Eocene, utilising records from northwest China and Myanmar. The role of

110   Qinghai-Tibetan uplift also remains unclear, with contrasting models of plateau evolution supported by various

111   tectonic, isotopic, modelling, and biological evidence (e.g., Mulch and Chamberlain, 2006; Rowley and Currie,

112   2006; Ding et al., 2014; Li et al., 2015; Jin et al., 2018; Botsyun et al., 2019; Su et al., 2019; Valdes et al., 2019;

113   Shen and Poulsen, 2019 and see summaries in Spurlin et al., 2005; Wang et al., 2014; Spicer, 2017).

114   Accordingly, further stratigraphic and paleoenvironmental studies of the sedimentary successions within these

115   basins are necessary to provide clarification on local vs. regional climatic changes experienced as a result of

116   uplift, global cooling, and progressive aridification in Central Asia during the Paleogene.

117   The location of the Nangqian Basin on the east-central part of the TP provides an ideal locality for testing

118   the influence of these mechanisms on Asian palaeoenvironments and climates. We selected the Ria Zhong (RZ)

119   section in the Nangqian Basin for palynological analyses, and correlated this section with previous studies from

120   this and other TP basins. These new results better constrain the biostratigraphy of Paleogene successions across

121   the plateau, and provide new information on the depositional environment, and elevational and climatic changes

122   in eastern Tibet during the Eocene. We further synthesise results previously published in Chinese journals,

123   making these results accessible for an international audience.

124

125   **2.   Geological background, stratigraphy and lithofacies**

126   The Nangqian Basin is located on the border between the Qinghai Province and Tibet Autonomous Region

127   at an elevation of approximately 4500–5000 m and characterized by a continental seasonal monsoon climate,

128   with long, cold winters, and short, rainy, and cool to warm summers (Yuan et al., 2017). Most of the annual

129   precipitation occurs from June to September, when on average, most days in each month experience some

130   rainfall (Qinghai BGMR, 1991). The region presently hosts alpine steppe and meadow (Fig. 1) characterised by

131   Cyperaceae, Asteraceae, Amaranthaceae, and Poaceae, as well as conifer and broad-leaved forests dominated by

132 conifers such as *Pinus*, *Picea*, *Abies*, *Tsuga*, and deciduous angiosperms such as *Quercus* (oak) and *Betula*

133 (birch) although intensive logging has markedly contracted these forests to steep slopes and remote areas

134 (Herzschuh, 2007; Baumann et al., 2009).

135 Although the timing of the Indo-Asian collision remains uncertain (e.g., Xia et al., 2011; Zhang et al.,

136 2012; Wang et al., 2014), its initiation formed north-eastward extrusion facilitated by motion along a series of

137 contraction deformation and strike-slip faults in eastern Tibet, including the Yushu–Nangqian thrust belt and the

138 Jinshajiang strike-slip fault system (Fig. 1; Hou et al., 2003; Yin and Harrison, 2000; Spurlin et al., 2005). The

139 Nangqian Basin is one of four sedimentary basins in the Nangqian-Yushu region that formed during Paleogene

140 contraction (Horton et al., 2002), ~80 km-long in S–N direction, and 15 km-wide in E–W direction, and situated

141 in the eastern part of the Qiangtang terrane (Fig. 1; Hou et al., 2003). The tectonic evolutionary history of the

142 area includes an early stage extrusion thrust foreland basin, a middle stage strike-slip foreland basin, and the late

143 stage extrusion strike-slip foreland basin (Wang et al., 2001, 2002; Mao et al., 2010; Jiang et al., 2011).

144 Paleozoic, Mesozoic, and Paleogene sedimentary rocks exposed along the Yushu-Nangqian traverse

145 include Carboniferous–Triassic marine carbonates and minor clastic units overlain by Jurassic, Cretaceous, and

146 Paleogene red beds (Liu, 1988; Qinghai BGMR, 1991). The southern area mainly comprises the Carboniferous

147 Zhaduo Group (C^1zd), whereas the northern area is dominated by younger strata comprising the Upper Triassic

148 Jieza Group (T^3jz; Qinghai BGMR, 1991). Our study concentrated on the Cenozoic gypsum-bearing Gongjue

149 Formation, which unconformably overlies Carboniferous–Triassic rocks and may be conformable with

150 underlying Upper Cretaceous strata (Qinghai BGMR, 1983a, 1983b, 1991). It is divided into five lithological

151 units (Eg^1–Eg^5), from bottom to top (Du et al., 2011). Eg^1 comprises shallow lacustrine facies reaching a

152 thickness of ca. 400 m, which lie unconformably on a basement of Carboniferous–Permian sedimentary rocks.

153 The strata in units Eg^2, Eg^4, and Eg^5 were mainly formed in an alluvial environment with rapid sedimentation

154 rates, with strata reaching a thickness of ca. 530 m, 1100 m, and 2500 m respectively.

155 The focus of this study is the Eg^3 unit which has a more complex depositional history; it is the thickest

156 (reaching 3500 m) of the five units, and the most widely distributed unit in the Nangqian Basin. Eg^3 is divided

157 into three members: 1) the Ri'Anongguo conglomerate member, which reaches a thickness of approx. 1300 m;

158 2) the Dong Y'ru sandstone member with limestone beds, which reaches a thickness of 700–1000 m; and 3) the

159 uppermost Gouriwa member, comprising mudstones (generally developed as red beds) intercalated with gypsum

160 and reaching 900–1200 m in thickness (Wang et al., 2002). This latter member has been interpreted as being

161 deposited in a fluviolacustrine environment under a range of climatic conditions (Wang et al., 2001, 2002; Jiang

162 et al., 2011). Note that the stratigraphic framework for the Gongjue Formation described in Yuan et al. (2017) is

163 incorrect, referring to the three members above as comprising the entire Gongjue Formation instead of only the

164 Eg³ unit within the Gongjue Formation; we correct this here based on the descriptions of Wang et al. (2001,

165 2002) and Du et al. (2011). Based on palynological analyses and ostracod assemblages, these mudstone-

166 dominated successions of the (Eg³ unit) have been dated as late Eocene to Oligocene in age (Wei, 1985; Yuan et

167 al., 2017), which is corroborated by 38–37 Ma ^{40}Ar/^{39}Ar ages from interbedded volcanic rocks in the uppermost

168 strata of the Nangqian Basin (Spurlin et al., 2005).

169   Though few palynological data currently exist from the Nangqian Basin (Wei, 1985; Yuan et al., 2017),

170 palynology has been extensively applied for biostratigraphic purposes, as well as to infer Cenozoic climatic

171 changes, in basins across the TP, including the Qaidam Basin (Xu et al., 1958; Zhu et al.,1985; Wang et al.,

172 1999; Sun et al., 2005; Lu et al., 2010; Ji et al., 2011; Miao et al., 2011, 2012, 2013a; Cai et al., 2012; Herb et

173 al., 2015; Wei et al., 2015), Xining Basin (Dupont-Nivet et al., 2008; Miao, 2010; Hoorn et al., 2012; Miao et

174 al., 2013b; Bosboom et al., 2014), Hoh Xil Basin (Liu et al., 2003; Miao et al., 2016), Tarim Basin (Sun et al.,

175 1999; Zhu et al., 2005; Bosboom et al., 2011; Wang et al., 2013), Jianchuan Basin (Li L. et al., 2019), and the

176 Xigaze region of Tibet (Li et al., 2008). Most of these studies are limited to the sedimentary successions within

177 the foreland basins of the northern TP, rendering it important to gather further data on central Tibetan basins that

178 preserve a complex sequence of Cenozoic deformation in relation to the Indo-Asian collision zone (Spurlin et

179 al., 2005). Furthermore, correlation of the above-mentioned northern successions with our new section from the

180 Nangqian Basin (presented in Section 5.1) is valuable for advancing understanding of differences in vegetational

181 composition across the TP, as well as the paleoenvironmental and climatic signals recorded by these ecosystems.

182

183 **3.   Materials and Methods**

184   In this study, the RZ section located in the northwestern part of the Nangqian Town (N32°12'10",

185 E96°27'19.42", altitude 3681 m) was sampled for sedimentological and palynological analyses (Fig. 21). The

186 RZ section is a ca. 260 m thick portion of the Gongjue Formation where it represents the uppermost Gouriwa

187 mMember of the Eg³ unit. The sediments mainly comprise lacustrine facies represented by red mudstones and

188 siltstones, intercalated with gypsum beds. A more detailed description of the sedimentology, geochemistry, and

189 palynofacies of the section are presented in a separate manuscript (Yuan et al., in prep.submitted). A total of 71

190 palynological samples were collected from mudstones or fine-grained siltstones.
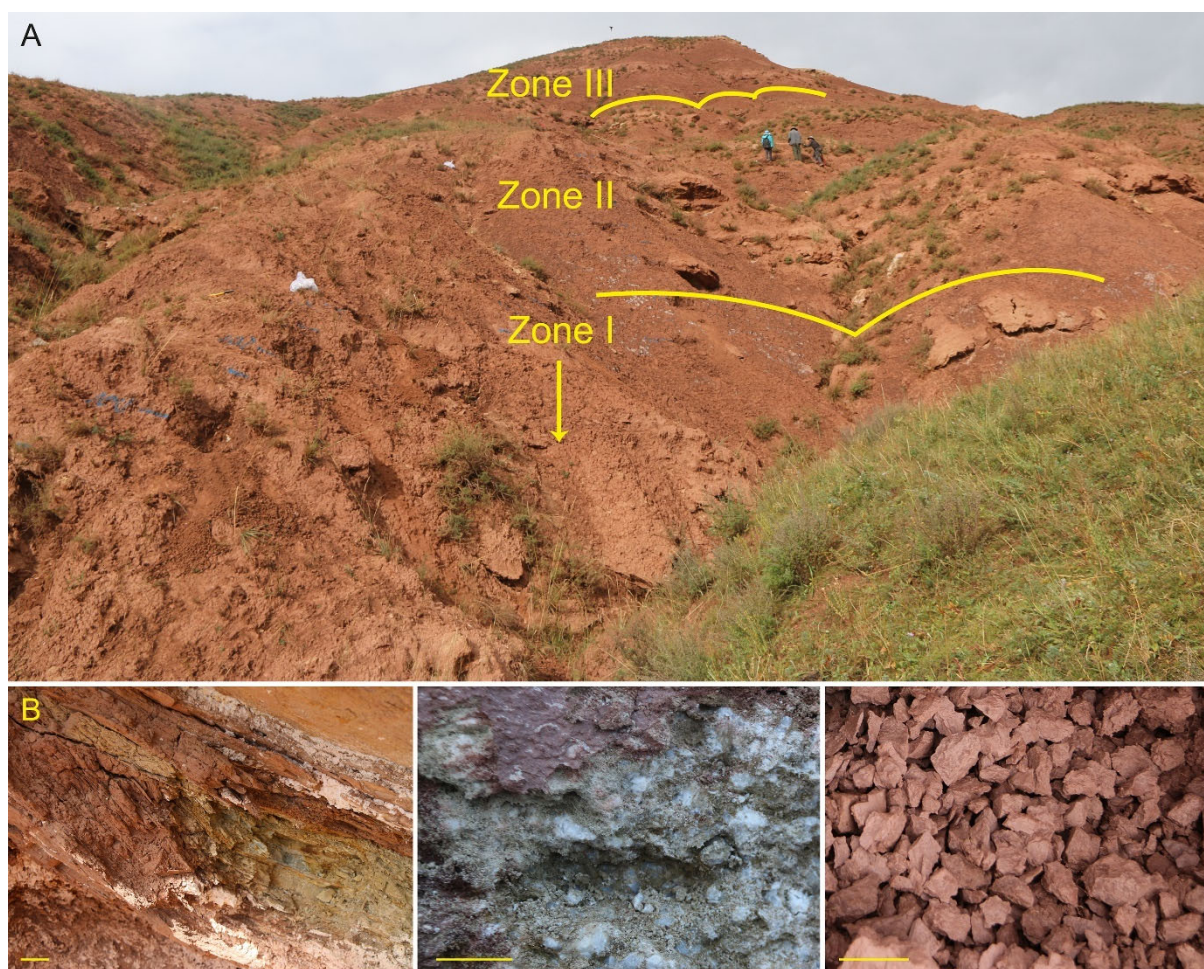
7

Figure 2A. Field photograph of the newly sampled Ria Zhong (RZ) section with palynological zones marked. The section is located in the Nangqian Basin, Yushu area, Tibet (N32° 12' 10", E 96° 27' 19.42", altitude 3681 m), and represents the uppermost Gouriwa member of the Eg³ unit in the Cenozoic Gongjue Formation. The lithostratigraphy and geochemistry of the RZ section are further described in Yuan et al. (submitted). B. Field photographs showing representative lithologies in the RZ section, from left: intercalated siltstone and mudstone; massive gypsum; silty mudstone. Scale bar – 5 cm.

Table 1. Lithologies of the palynological zones identified within the Ria Zhong (RZ) section in the Nangqian Basin, Yushu area, Tibet. Information is given on the stratigraphic horizons of each zone, its dominant lithologies, and the total number of productive palynological samples that were obtained.

Zone	Depth (m)	Dominant lithologies	Productive samples
III	101–16	Silty mudstones and siltstones with thin gypsum beds	2
II	147–101	Mudstones, nodular mudstones and silty mudstones with thin gypsum beds	2
I	251–147	Mudstones and gypsum	17

203   The samples were first treated with 36% HCl and 39% HF to remove carbonates and silicates and then

204   sieved through a 10 μm nylon mesh. Subsequently, the residue was density separated using ZnCl2 (density =

205   2.1). The organic residue was mounted on microscopic slides in glycerin jelly. All slides were examined at the

206   Swedish Museum of Natural History under a Leica light-microscope (OLYMPUS BX51), and micrographs were

207   taken of selected specimens. As is standard for palynostratigraphic studies, we used primarily light microscopy

208   (LM) to identify, count, and photograph palynomorphs present in the samples. An ESEM FEI Quanta FEG 650

209   scanning electron microscope (SEM) was used to obtain additional detailed surface images of *Ephedripites*

210   *(Ephedripites), Ephedripites (Distachyapites),* and other key species. Slides and residues are hosted at the

211   Swedish Museum of Natural History, Stockholm, Sweden.

212   From each of the 21 productive samples > 200 grains were identified and counted, and the pollen diagrams

213   (Fig. 3, Fig. S1 and Fig. S2) plotted using TGView© and Tilia© 2.0 software (Grimm, 1991). We assigned fossil

214   pollen taxa to Ecological groups or Plant Functional Types (PFTs) according to their correspondence with

215   nearest living relatives (NLR) in modern Asian biomes (following the taxon-to-NLR assignmentsapproach of

216   Hoorn et al., 2012). PFTs are shown in the supplementary dataset of Yuan & Barbolini (2020) as well as Fig. S1

217   and S2. Statistical analysis of the palynological assemblages was conducted using CONISS (Constrained

218   Incremental Sums of Squares cluster analysis), a multivariate agglomerative method for defining zones

219   hierarchically (Grimm, 1987). A stratigraphically constrained analysis was performed on pollen-percentage

220   values with square root transformation (Edwards and Cavalli Sforza's chord distance) which up-weights rare

221   variables relative to abundant ones, and is therefore particularly appropriate for pollen datasets (Grimm, 1987).

222   Results of the CONISS ordination on all taxa were presented as a dendrogram onto the pollen diagram (Fig. S1),

223   and the ordination was then repeated to test the robustness of the stratigraphic zones by excluding the "Other /

224   Unknown / Unresolved NLR" ecological group. Very similar zones were retained in the new cluster analysis

225   (Fig. S2), increasing confidence that these zones represent true changes in vegetation and climate dynamics

226   recorded throughout the section. Both CONISS ordinations were used in conjunction with the taxonomic and

227   quantitative composition of the palynological assemblage, in order to demarcate zones and subzones within the

228   section.

229

230   **4. Results**

231   Recovery of palynomorphs was generally poor, particularly in the upper part (0–147 m) of the section.

232   Although there is no direct linkage between the productivity of pollen samples and lithofacies, evidence of

233   increasing aridity is preserved in the upper part of the section through both the palynological and

234   sedimentological records. Accordingly, vegetation biomass was likely lower in these more arid environments,

235   and extended exposure on the landscape before burial can destroy palynomorphs; both of these factors are likely

236   contributors to the lower productivity observed. Inwith total, only 21 productive samples were obtained out of

237   thefrom 71 processed samples, indicating a productivity ratio of 30%. Nevertheless, individual well-preserved

238   palynological assemblages were recovered throughout the section, enabling a representative portrayal of

239   vegetation changes through time to be reconstructed. In total 26 spore and 81 pollen taxa (5 gymnosperm and 76

240   angiosperm morphospecies) were able to be identified, which are illustrated (Plate I, II, III) and grouped into

241   seven different Plant Functional Types (PFTs) that represent various ecological groups (Fig. 3). Overall trends

242   for the RZ section include rare conifers and a general dominance of steppe-desert pollen in all zones. Ferns are

243   abundant and diverse, particularly in the lower part of the section (Zone I), while temperate and warm broad-

244   leaved forest are relatively diverse and present throughout, but not particularly abundant in any zone. Steppe-

245   desert pollen decreases concurrently with a spike in tropical forest pollen in one sample fromin Zone II, and then

246   resurges to dominance in Zone III. Palynological zones are marked on the field photograph of the RZ section

247   (Fig. 2) and plotted on the pollen diagrams (Fig. 3, Fig. S1 and Fig. S2).

248   While the generally high proportion of spores suggests a significant proportion of local deposition (at site),

249   as a whole the palynological assemblages are taken to reflect the regional vegetation, and may also include some

250   taxa that are prone to longer-distance transport. These latter taxa are mostly trees, and are normally present in

251   small percentages except for *Pinus*, which can comprise 10–50% in the palynological records of deserts and

252   steppe–deserts (but is extremely rare in our section; Ma et al., 2008; Hoorn et al., 2012). Studies on the

253   correspondence between the modern pollen rain and regional vegetation on the Tibetan Plateau indicate

254   generally good agreement, and confirm that the use of palynology for palaeoenvironmental reconstruction in

255   deep time is therefore also appropriate (Cour et al., 1999; Li et al., 2020).
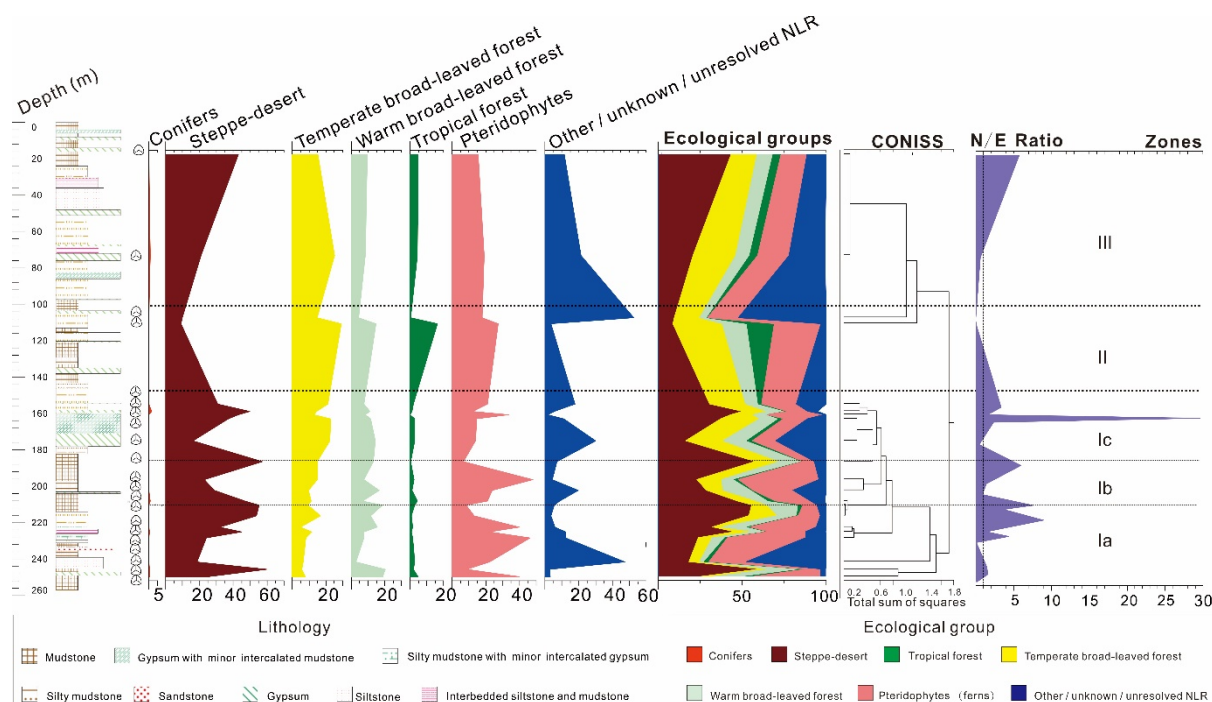
256

Figure 3: Cumulative pollen summary diagram of the Ria Zhong (RZ) section in the Nangqian Basin, Yushu area, Tibet, with palynomorph percentages of the total pollen sum plotted on the x-axis, and zones and subzones based on CONISS ordinations. Pollen taxa are grouped in Plant Functional Types (PFTs) according to their correspondence with nearest living relatives (NLR), indicated in the legend. Some taxa have multiple or unresolved botanical affinities, and are thus assigned to the "Other / unknown / unresolved NLR" group. Productive horizons are indicated by a small trilete spore to the right of the simplified section log. The *Nitraria/Ephedra* (N/E) pollen ratio is plotted in purple, with a dashed line indicating the transition point between desert/semi-desert ecosystems (< 1) and steppe-desert (> 1).

4.1 Stratigraphic zonation based on palynology

Based on results of two CONISS ordinations combined with the taxonomic and quantitative composition of the palynological assemblage (see Methods section; Fig. 3, Fig. S1 and Fig. S2), the succession was divided into three zones (I, II, III) of which Zone I was further divided into three subzones (a, b, c), all of which demonstrate unique vegetation dynamics within that zone. Important trends for each zone and subzone are described below. The zone boundaries are positioned at the upper limit of the samples that mark each boundary. A complete overview of the raw counts, percentages and arithmetic means are given in the supplementary information.

Plate I: Light micrographs of selected pollen grains and spores from the Ria Zhong (RZ) section, Nangqian Basin.

Scale bar – 10µm. 1-12. *Nitrariadites/Nitraripollis*. **13-20.** *Meliaceoidites*. **21-25.** *Qinghaipollis*. **26-32.** *Rhoipites*. **33-36.**

Labitricolpites. **37-45.** *Quercoidites*. **46.** *Quercoidites minutus*. **47-51.** *Rutaceoipollenites*. **52-54.** *Momipites*. **55-58.**

Fupingopollenites. **59-61.** *Ilexpollenites*. **62.** *Aceripollenites*. **63-67.** *Euphorbiacites*. **68-69.** *Faguspollenites*. **70.**

282　*Retitricolporites.* **71.** *Chenopodipollis.* **72.** *Echitriporites* **sp. 73.** *Sporopollis.* **74.** *Caprifoliipites / Oleoidearumpollenites***?.**

283　**75-76.** *Pterisisporites.* **77. Unidentified baculate spore. 78.** *Liliacidites.* **79-80.** *Pterisisporites.* **81.** *Taxodiacites.* **82-83.**

284　*Deltoidospora.* **84.** *Lycopodiumsporites.* **85.** *Spinizonocolpites.* **86-88.** *Verrucosisporites.* **90.** *Lygodiumsporites.*

285

286

288　**Plate II: Light micrographs of ephedroid pollen from the Ria Zhong (RZ) section, Nangqian Basin. Scale bar – 10μm.**

289　**A.** *Ephedripites (Distachyapites) cheganica.* **B.** *Ephedripites (Distachyapites) fusiformis.* **C1-C4.** *Ephedripites*

290　*(Distachyapites) megafusiformis.* **D1-D2.** *Ephedripites (Distachyapites) eocenipites.* **E1-E3.** *Ephedripites (Distachyapites)*

291　*nanglingensis.* **F.** *Ephedripites (Distachyapites) obesus.* **G.** *Ephedripites (Ephedripites) bernheidensis.* **I.** *Ephedripites*

292　*(Ephedripites)* **sp. 2 (Han et al., 2016). K.** *Ephedripites (Ephedripites)* **sp. b. H.** *Ephedripites (Ephedripites)*

293　*montanaensis.* **J.** *Ephedripites (Ephedripites)* **sp. a. L.** *Steevesipollenites cf S. binodosus.* **M.** *Steevesipollenites*
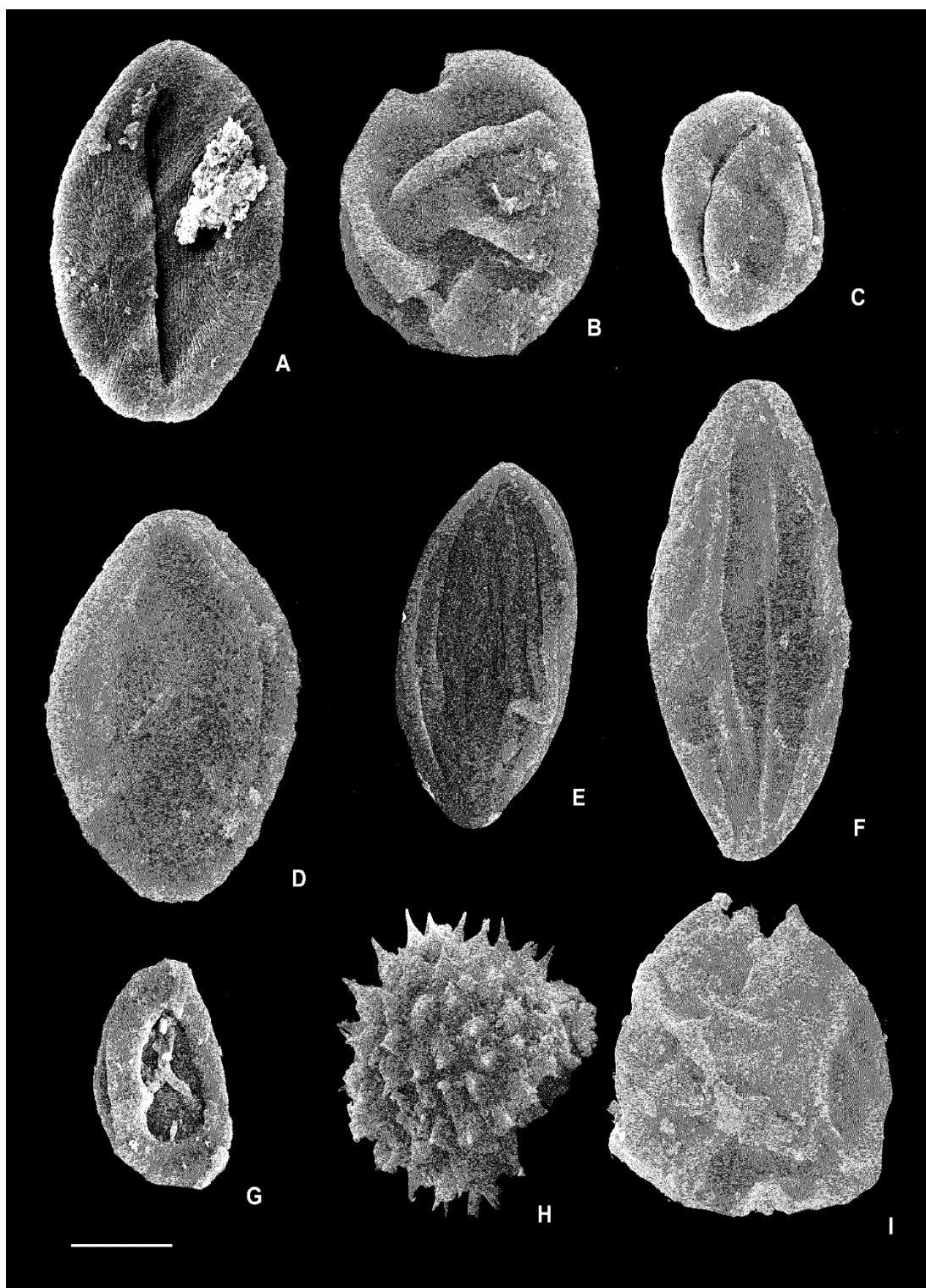
294　*jiangxiensis.*

295

Plate III: Scanning Electron Microscope (SEM) photographs of selected fossil taxa in the Ria Zhong (RZ) section, Nangqian Basin. Scale bar – 10μm. A, B, C. *Nitrariadites/Nitraripollis.* **D.** *Retitricolporites.* **E.** *Ephedripites (Ephedripites) sp. 2 (Han et al., 2016).* **F.** *Ephedripites (Distachyapites) eocenipites.* **G.** *Pterisisporites.* **H. Unidentified baculate spore. I.** *Momipites.*

4.1.1 Zone I (17 samples, 251–147 m)

Conifers in this zone are rare, represented only by *Taxodiacites* (Cupressaceae) and *Tsugaepollenites* (Pinaceae), and never comprising more than 3%. The assemblage is dominated by steppe-desert taxa, which together comprise nearly 40% and include numerous types of *Ephedripites* (Plate II), *Nitrariadites/Nitraripollis*, and *Qinghaipollis*, together with more rare xerophytic taxa such as *Chenopodipollis* and *Nanlingpollis*. The second most abundant group is the Pteridophytes (ferns), which is also the most diverse of all the groups represented in the RZ section. Broad-leaved forest forms a minor component of the palynological record, with warm forest being more abundant than temperate forest and represented primarily by *Rutaceoipollenites*. Tropical forest pollen is rare, and includes *Spinizonocolpites* and *Fupingopollenites*. Some pollen types have unresolved botanical affinities or affinities with multiple ecological groups, and these are grouped separately but do not provide ecological information.

Zone I is divided into three subzones on the basis of abundance patterns among particular palynomorph taxa. Subzone **Ia** (9 samples, 251–209 m) is unique in that *Ephedripites* (steppe-desert group), *Cupuliferoipollenites* (temperate broad-leaved forest), and *Rutaceoipollenites* (warm broad-leaved forest) are more abundant than in other subzones of Zone I, while *Momipites / Engelhardthioipollenites* (warm broad-leaved forest) is less abundant, and *Aceripollenites + Faguspollenites* (temperate broad-leaved forest) are very rare compared to the remainder of Zone I. Of the entire section, *Caryophyllidites* (steppe-desert) only occurs in **Subzone Ib** (3 samples, 209–187 m), which also records a spike of *Momipites/Engelhardthioipollenites* (warm broad-leaved forest). **Subzone Ic** (5 samples, 187–147 m) contains the greatest proportion of *Nanlingpollis* (steppe-desert) in the entire section, as well as spikes of *Aceripollenites + Fraxinoipollenites* (temperate broad-leaved forest), while *Qinghaipollis* (steppe-desert) and ferns decrease in this subzone.

4.1.2 Zone II (2 samples, 147–101 m)

No conifer pollen occurs in this zone, and on average, the steppe-desert taxa *Ephedripites* (gymnosperm)*, Nitrariadites/Nitraripollis* and *Qinghapollis* (angiosperms) are far less abundant than in other parts of the section (average 9% in Zone II vs 38% (Zone I) and 32 % (Zone III)). However, a spike in the ancestral (old) *Ephedra* type is observed during Zone II, which is not observed in the other zones or later in the Eocene (Yuan et al., 2017). Notably, tropical forest pollen increases markedly in one sample from this zone (as regional input), comprising mostly *Fupingopollenites*, while temperate broad-leaved forest (*Aceripollenites*, cf. *Caprifoliipites*) and warm broad-leaved forest (*Rutaceoipollenites*) are also more prevalent. Pollen of unknown or multiple

affinities is higher in this zone, and reflected by spikes of *Labitricolpites* and *Rhoipites*. A low recovery of productive samples was obtained from this zone, and the above-described trends may thus reflect an incomplete picture of environmental changes during this interval.

4.1.3 Zone III (2 samples, 101–16 m)

Conifers in this zone are very rare, represented only by *Tsugaepollenites*. Steppe-desert taxa again dominate this zone, with *Nitrariadites/Nitraripollis* increasing steadily through the section. Temperate broad-leaved forest is now much more common than warm broad-leaf or tropical forest pollen, while ferns are least common in this zone but still plentiful. A low recovery of productive samples was obtained from this zone, and the above-described trends may thus reflect an incomplete picture of environmental changes during this interval.

5. Discussion

5.1 Age assignment

Age constraints for the RZ section are provided by the K–Ar ages from shoshonitic lavas and felsic and porphyry intrusions that are either interbedded with, or unconformably overlie, the lacustrine to alluvial Nangqian strata. Emplacement ages across the Nangqian Basin vary between 32.04–36.5 Ma (Deng et al., 1999); 37.0 ± 0.2 Ma–38.2 ± 0.1 Ma (Spurlin et al., 2005); 37.1–37.8 Ma (Zhu et al., 2006); and 35.6 ± 0.3–39.5 ± 0.3 Ma (Xu et al., 2016). In the latter study, zircon U–Pb age data were derived from felsic intrusions sampled at two localities in the Nangqian Basin (Boza and Nangqian). The syenite porphyries from the Boza area (further south of the RZ section) show an emplacement age of 35.58 ± 0.33 Ma, while the monzonite porphyries from the Nangqian area (just southeast of the RZ section) have older magmatic emplacement ages, ranging from 39.5 ± 0.3 Ma to 37.4 ± 0.3 Ma. As this age range is broadly coeval with the age of the mafic volcanic rocks in the Nangqian Basin (37.0–38.2 Ma; Spurlin et al., 2005) as well as the age range obtained by Zhu et al. (2006), here we consider ~37–38 Ma to represent a minimum age for the RZ section. This is also congruent with palynological evidence for the overall age of the sampled strata (Fig. 4), which is discussed in more detail below.

The assemblage from the RZ section is very similar to those from the Yang Ala section in the Nangqian Basin, dated as late Eocene (Yuan et al., 2017), the Eocene Wuqia assemblage (site 98) from the west Tarim Basin (Wang et al., 1990a; 1990b), the late middle Eocene–late Eocene assemblage from the upper Niubao

362 Formation, Lunpola Basin (Song and Liu, 1982; Li J.G. et al., 2019), and the Bartonian (41.2–37.8 Ma) part of

363 the palynological record in the Xining Basin (Dupont-Nivet et al., 2008; Hoorn et al., 2012; Han et al., 2016).

364 Specifically, the absence of *Classopollis*, *Exesipollenites*, and *Cycadopites* combined with the predominance of

365 *Nitrariadites/Nitraripollis* and *Ephedripites* pollen, and the presence of the middle Eocene–Neogene genus

366 *Fupinggopollenites* (Liu, 1985), indicates that the RZ section cannot be older than middle Eocene (Fig. 4). It is

367 also unlikely to be of latest Eocene age or younger due to the lack of significant conifers that become more

368 common approaching the Eocene–Oligocene Transition (Hoorn et al., 2012; Page et al., 2019; Fig. 4). Specific

369 ranges and abundance patterns of these and other key taxa within Eocene Tibetan basins (Fig. 4; Fig. 5) enable

370 the age of the section to be better constrained, which is explored in greater detail below.

371　*Ephedra* is a gymnosperm shrub with the oldest macrofossils from the Early Cretaceous (Bolinder et al.,

372 2016; Han et al., 2016) but the genus is probably older, dating to the Triassic (Yang, 2002; Sun and Wang, 2005)

373 or even the Permian (Wang, 2004) based on the ephedroid pollen record. Its current distribution is limited

374 primarily to arid and semiarid regions of the world (Stanley et al., 2001), and the fossil pollen representative,

375 *Ephedripites*, is widespread in Cenozoic evaporates, indicating the xerophytic nature of this genus (Sun and

376 Wang, 2005). The Xining Basin in northern Tibet records a particularly time-extensive section with good age

377 control (Dupont-Nivet et al., 2008, 2008; Hoorn et al., 2012; Meijer et al., 2019) that reveals a detailed pattern

378 of changes in *Ephedripites* pollen during the middle–late Eocene. After 38.8 Ma, *Ephedripites* comprised ca.

379 20–60% of the total palynological composition in the Xining Basin, with a predominance of the derived type,

380 *Ephedripites* subgen. *Distachyapites* (Han et al., 2016). Prior to this (ca. 41–38.8 Ma), the record comprised a

381 mix of the derived type, the ancestral type (*Ephedripites* subgen. *Ephedripites*), and another ephedroid genus,

382 *Steevesipollenites* (Han et al., 2016; Bolinder et al., 2016). A similar pattern is observed in the Nangqian Basin,

383 with a spike of the ancestral type of *Ephedra* only recorded in Zone II, and not observed in the rest of the RZ

384 section or elsewhere in the Nangqian Basin (Yuan et al., 2017). This suggests a correlation between Zone I of

385 the Xining Basin with Zone II of the RZ section (Fig. 5). As it is possible that the change in *Ephedripites*

386 diversity may not have occurred across Tibet simultaneously (i.e., at ~39 Ma), we suggest that this most likely

387 constrains the age of the RZ section to late Eocene (Bartonian; 41.2–37.8 Ma).

388

389
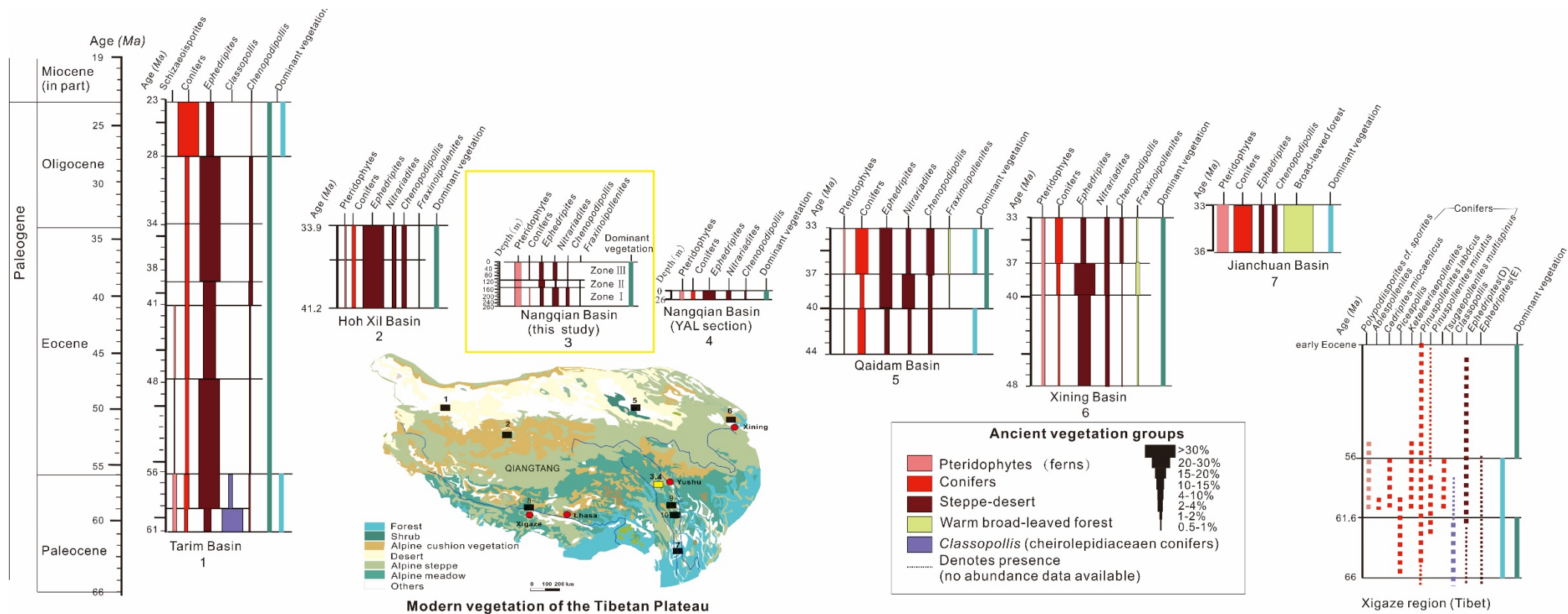
Figure 43: Palynozonation of the Paleogene successions across the northern, central, and southern TP, with numbers under each section indicating the associated basin: 1. Tarim Basin (Wang et al., 1990a; 1990b); 2. Hoh Xil Basin (Miao et al., 2016); 3, 4. Nangqian Basin (this study; Yuan et al., 2017). 5. Qaidam Basin (Lu et al., 1985; Zhang et al., 2006; Miao et al., 2016); 6. Xining Basin (Wang et al., 1990a; 1990b; Hoorn et al., 2012); 7. Jianchuan Basin (Wu et al., 2018); 8. Xigaze Basin (Li et al., 2008). The dominant ancient vegetation reconstructed from palynological assemblages is shown to the right of each section. Modern vegetation map redrawn from Baumann et al. (2009).

394
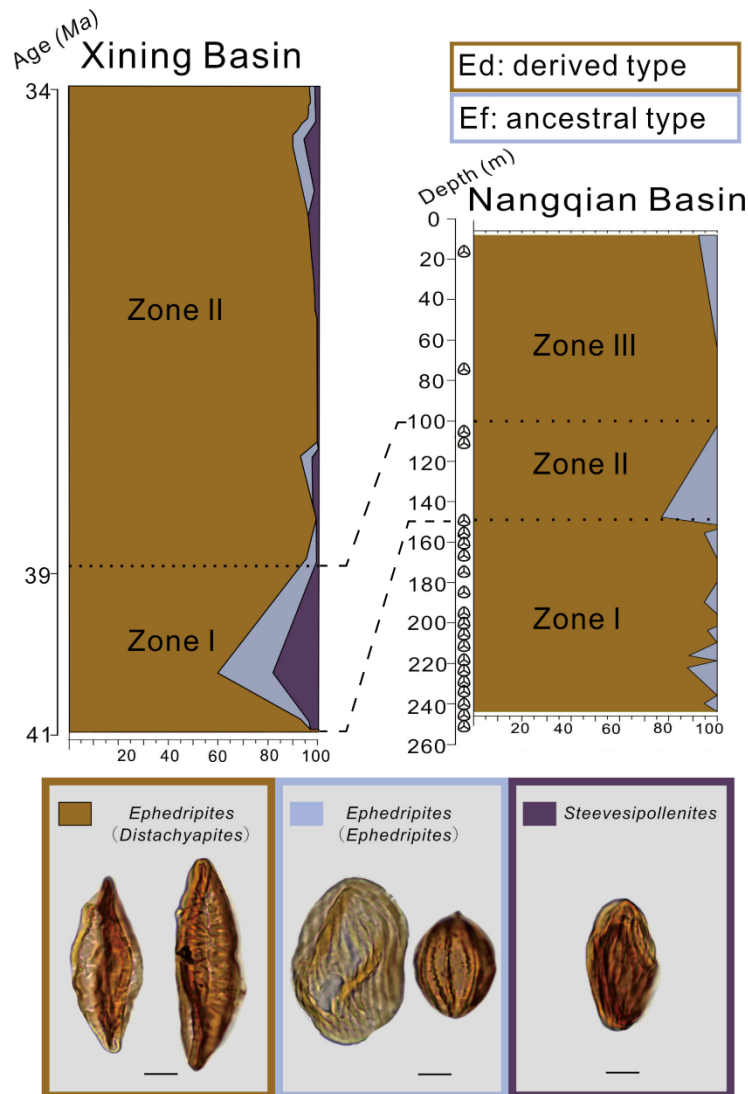
Figure 54: Eocene ephedroid pollen composition in the Xining (northeastern TP) and Nangqian (east-central TP)
basins, illustrating the distributions of *Ephedripites* subgen. *Ephedripites* (ancestral type; "Ef"), *Ephedripites* subgen.
***Distachyapites* (derived type; "Ed"), and *Steevesipollenites*. Productive horizons for the R~~h~~ia Zhong (RZ) section are**
indicated by a small trilete spore to the right of the marked depths.

In addition to the proportions of the ancestral vs. derived type of *Ephedripites*, a significant spike in

tropical forest pollen in one sample at this time, combined with a large decrease in steppe-desert pollen, suggests

that Zone II of the RZ section reflects a temporary warming interval in the Eocene. Although the increase in

tropical forest taxa in in one sample from this zone does not indicate an actual biome shift in the Nangqian

region from "steppe" to "tropical forest", it suggests a change in regional climate through increased input of

regional tropical taxa. This could possibly be concurrent with the MECO (~40 Ma), a transient warming event

407   that preceded rapid aridification in Central Asia (driven primarily by proto-Parathethys sea retreat; Kaya et al.,

408   2019). This interval is followed by a change in lithofacies (decreasing thickness of gypsum beds) and an

409   increase in steppe-desert pollen records in northwestern China (Bosboom et al., 2014). Similar trends are also

410   observed in the Nangqian Basin (Fig. 3), suggesting a possible correlation. However, it must be considered that

411   the upper zones of the RZ section yielded a low number of samples (Zone II and III each comprise only 2

412   samples), and the tropical forest spike is only present in one of these samples. This places statistical limitations

413   on the interpretations that can be drawn, therefore further investigations should be made in Nangqian and other

414   parts of Tibet to corroborate this finding. Accordingly, for the moment we do not date the RZ section on the

415   basis of a tentative correlation to the MECO at ~40 Ma; however, available evidence does suggest that the spike

416   of tropical forest represents a temporary shift in regional climate. The palynomorphs from these samples were

417   not degraded or compressed to a greater degree than palynomorphs from the rest of the section, and of a similar

418   colour and appearance, suggesting it is unlikely that the pollen in Zone II represents reworking or

419   contamination. Furthermore, the increase in tropical forest taxa is accompanied by a large decrease in steppe-

420   desert pollen which is not observed in the other zones of this section (average 9% steppe-desert pollen in Zone II

421   vs 38% (Zone I) and 32 % (Zone III)), nor later in the Eocene in the Nangqian Basin (Yuan et al., 2017). This

422   further indicates a temporary shift in the regional climate to warmer and wetter at this time.

423   In northern Tibet, Pinaceae (conifers) abruptly increased in the palynological record at 36.55 Ma (Page et

424   al., 2019), which is not observed in the RZ section. The rare conifers in this latter assemblage are in accordance

425   with the minimum depositional age constraints of ~37–38 Ma from overlying volcanic rocks. In conjunction

426   with the palynostratigraphic correlations from across Tibet (Fig. 4), as well as the change in the proportions of

427   the ancestral vs. derived type of *Ephedripites* (Fig. 5), the age of the complete section is proposed to be

428   Bartonian (41.2–37.8 Ma; Fig. 4; Fig. 5).

429

430   **5.2 Paleoclimate**

431   The RZ section records three distinct palaeofloras in east-central Tibet that evolved in response to changing

432   climate in the Eocene (Fig. 6). During deposition of Zone I, the climate was warm, and vegetation was

433   characterised by steppe-desert shrubs, diverse ferns, and a lesser component of temperate and warm broad-

434   leaved forest. Interestingly, prominent vegetation groups with very different moisture requirements existed

435   within a limited distance of each another in the Nangqian area. A very diverse and abundant pteridophyte (fern)

436   community, as well as conifers such as *Taxodiacites* and *Tsugaepollenites* would have required higher humidity

437 (Liu et al., 2012; Kotthoff et al., 2014), but the abundant halophytic and xerophytic steppe-desert vegetation

438 would likely only have been competitive in arid environments. The dominant plants belonging to these salt- and

439 drought- tolerant groups (*Nitraria* and *Ephedra*) grow today in Central Asian regions with MAP of 100mm or

440 less, and are also associated with arid palaeoenvironments through the Cenozoic (Sun and Wang, 2005).

441 Although the conifers (produced by cypress and *Tsuga*) could have been windblown from further distances, the

442 coexistence of such diverse and abundant ferns and steppe-desert vegetation in the landscape, PFTs with

443 opposing moisture requirements for competitiveness, has not been observed in other Tibetan basins to date

444 (Miao et al., 2016, Table 1), and therefore seems not to reflect conventional spatial patterning of less water-

445 dependant vegetation growing upland. Rather, it may suggest an environment with strongly seasonal

446 precipitation that would favour lush vegetation growth for a restricted interval and alternately, xerophytic

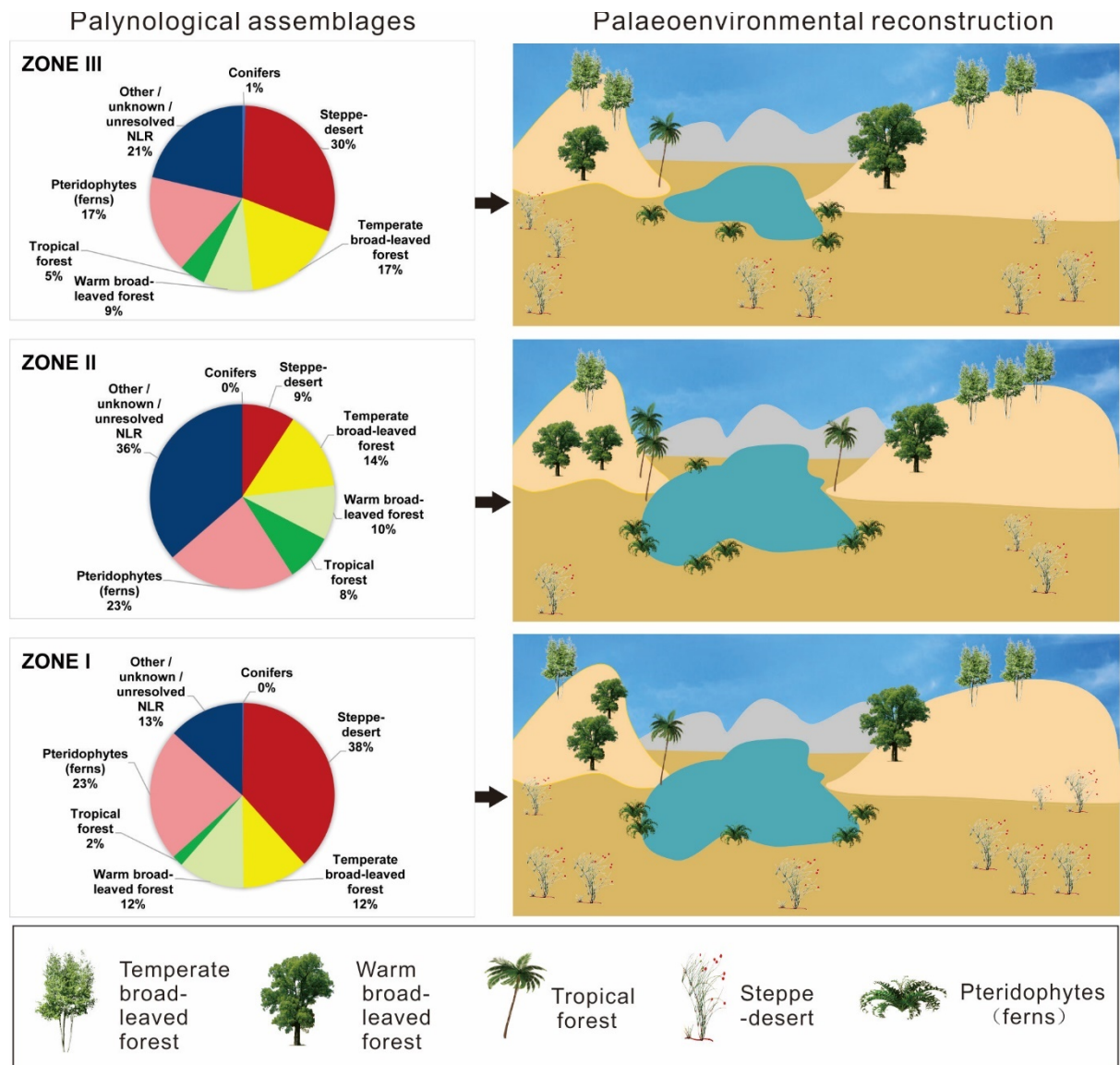447 vegetation during the dry season.

448

Figure 65: Palaeoenvironmental reconstruction of the Nangqian area, illustrating the three distinct floral assemblages recovered from the RZ section. Vegetation during deposition of Zone I was dominated by steppe-desert shrubs, which decreased sharply in Zone II in conjunction with a spike in tropical forest. Afterwards the basin became drier and steppe-desert vegetation again dominated the landscape.

Based on a comparison of existing palynofloral records with our new section, the northern regions of the plateau (Tarim, Qaidam, Hoh Xil, and Xining basins) were already significantly more arid than the central TP in the middle Eocene, having hosted greater proportions of xerophytic plants (Fig. 4). Therefore, precipitation in the greater Nangqian region would have been unlikely to derive from the westerlies, which served as the dominant moisture source northward of the central TP since at least the early Eocene (Caves et al., 2015). This suggests that the central TP could have instead been influenced by a southern monsoon system similar to the modern I-AM in the middle–late Eocene, although not to the degree experienced by southern Tibet, which

462   hosted greater proportions of forest and was likely more humid (e.g., Jianchuan Basin; Fig. 4). However, it

463   should be borne in mind that rainfall seasonality is not always a proxy for the existence of monsoons; although

464   leaf form is the preferred method for detecting monsoons in deep time climates (Spicer et al., 2017), the absence

465   of well-preserved fossil leaf assemblages from the Nangqian Basin to date prevents this comparison.

466   Furthermore, palynological records alone are not sufficient for detecting whether the nature of monsoons in the

467   Eocene was more similar to the present I-AM or South Asian Monsoon (SAM), which contributes mostly to the

468   moisture in the Nangqian region today (Li L. et al., 2019).

469   Our results indicate that the ~~temporary~~brief warming interval recorded in Zone II prompted a considerable

470   change in the vegetation in east-central Tibet, encouraging the temporary spread of (dry) forests in the region,

471   while steppe-desert vegetation contracted. Warming is reflected by an atypical spike in tropical forest, while a

472   warm broad-leaved forest spike in northeastern Tibet is coincident with the MECO (Hoorn et al., 2012; tropical

473   forest is exceedingly rare in the latter area during the middle–late Eocene). In order to estimate relative humidity

474   in arid environments such as these, the *Nitraria/Ephedra* (N/E) ratio can be used to distinguish between

475   desert/semi-desert (< 1) and steppe-desert (> 1; Li et al., 2005; Hoorn et al., 2012). Although both genera

476   occupy arid environments today, *Ephedra* is currently distributed primarily throughout deserts, semi-deserts and

477   grasslands globally (Stanley et al., 2001), while *Nitraria* is a relatively more humid steppe-desert taxon (Cour et

478   al., 1999; Sun and Wang, 2005; Jiang and Ding, 2008; Li et al., 2009; Zhao and Herzschuh, 2009).

479   In the RZ section, the proportion of temperate broad-leaved forest in relation to warm broad-leaf and

480   tropical forest became much greater in the upper part (Fig. 3), indicating a cooler climate in the late Eocene,

481   which matches cooling trends recorded by clumped isotopes both in the Nangqian Basin (Li L. et al., 2019) and

482   in the Xining Basin (Page et al., 2019). Importantly, the N/E ratio in the RZ section is lowest immediately

483   following the warming interval in Zone II (Fig. 3) and persists for an extended period, indicating rapid,

484   prolonged aridification. An overall expansion of steppe-desert vegetation is observed in Zone III, corresponding

485   with patterns observed on the northeastern TP in the late Eocene (Hoorn et al., 2012; Bosboom et al., 2014).

486   Accordingly, our vegetation results have implications for understanding the importance and extent of

487   aridification across Central Asia in the late Eocene, which was primarily driven by proto-Paratethys Sea

488   regression (Kaya et al., 2019). Ecosystem responses to this event on both the northeastern and east-central parts

489   of the TP demonstrates that aridification across the Asian continental interior in the late Eocene could have been

490   further-reaching than previously thought. Our findings show that after sea regression, westerly moisture supply

491   carried from the proto-Paratethys Sea was reduced as far as central Tibet. This provides further support for the

492   argument that this sea was a major source of moisture for the Asian interior, and thus a primary driver of Central

493   Asian climate during the Eocene (Bosboom et al., 2014; Bougeois et al., 2018; Kaya et al., 2019; Meijer et al.,

494   2019).

495   Long-term aridification in the late Eocene exerted further influence on vegetational composition in east-

496   central Tibet with regards to the proportions of the ancestral vs. derived types of *Ephedripites*. In modern and

497   Quaternary settings, this has been developed as a ratio to distinguish between desert and steppe-desert

498   environments, termed the *Ephedra fragilis*-type s.l./*Ephedra distachya*-type (Ef/Ed) ratio (whereby *E. fragilis*

499   represents the ancestral type and *E. distachya*, the derived type; Fig. 5). Tarasov et al. (1998) found the *E.*

500   *fragilis*-type s.l. to be common in arid climates with mean temperatures of the warmest month above 22°C.

501   Herzschuh et al. (2004) applied the Ef/Ed ratio to Holocene pollen spectra from the Alashan Plateau and tested

502   its reliability with a regional modern pollen dataset, finding Ef/Ed ratios > 10 in most samples from desert sites,

503   and values < 5 in most samples from the sites with more favourable climates (e.g., forest-steppe, steppe, and

504   alpine meadow).

505   In the middle–late Eocene of Central Asia, the ancestral type of *Ephedripites* never comprises more than

506   25% of the ephedroid pollen sum in northeastern Tibet while the derived type makes up at least 60% (Xining

507   Basin; Han et al., 2016 and Qaidam Basin; Zhu et al., 1985; Miao et al., 2013a; Jiuquan Basin; Miao et al.,

508   2008), and this also appears true for northwestern Tibet (Tarim Basin; Wang, et al., 1990b; Hoh Xil Basin; Miao

509   et al., 2016) and east-central Tibet (Yuan et al., 2017; this study). Therefore, Ef/Ed ratios > 10 (supposedly

510   indicative of desert ecosystems) are never observed, despite the N/E ratio indicating regular existence of deserts

511   or semi-deserts in northern Tibet (Zhu et al., 1985; Hoorn et al., 2012; Miao et al., 2016), and central Tibet

512   (Yuan et al., 2017; this study) in the Paleogene. Sedimentological evidence suggests the N/E ratio to be more

513   reliable for these deep time environments, with *Nitraria* and *Ephedra* pollen being widely distributed in

514   evaporites and red beds indicating deposition in arid or semi-arid climates (Sun and Wang, 2005). Therefore,

515   while pollen ratios appear to reflect reliable functions of climate and landscape change for modern and

516   Holocene settings (Li et al., 2010), our results identify possible contradictions between the N/E and Ef/Ed pollen

517   ratios. This indicates that further verification of these pollen ratios in modern settings and across larger spatial

518   scales is necessary for reliable palaeoenvironmental reconstructions in deep time.

519   A comparison of palynological assemblages across the Qinghai-Tibetan region indicates that vegetation has

520   changed markedly from the Paleogene to the present (Fig. 4). While the Nangqian region was dominated by

521   steppe-desert shrubs in the past, it now hosts primarily alpine biomes, as do the Hoh Xil and Xining basins. In

522 contrast, the Tarim and Qaidam basins are now significantly more arid than in the Eocene, and forest- and shrub-

523 steppe have been replaced with desert vegetation (Fig. 4). The Jianchuan Basin to the south was dominated by

524 mixed tropical-subtropical coniferous and broad-leaved forest (Wu et al., 2018), and is also forested today (but

525 with species of a less thermophilic nature). Similarly, the Markam and Gonjo basins host alpine meadow and

526 forest today; although detailed palynological records have not yet been recovered, macrobotanical fossils

527 suggest these areas were dominated by mixed broad-leaved and coniferous forest in the late Eocene–early

528 Oligocene (Su et al., 2018; Studnicki-Gizbert et al., 2008). The above changes indicate that late Paleogene and

529 Neogene topographic growth (creating new high-elevation biomes; Fig. 1A and B), the aridification of inner

530 Asia (Caves et al., 2014, 2016), and global cooling (Zachos et al., 2001; DeConto and Pollard, 2003; Pagani et

531 al., 2011) were all drivers of Cenozoic vegetation shifts across the TP.

532

533 **5.3 Elevational implications**

534 High-altitude conifers are rare in this particular record, although the high-elevation genus *Tsugaepollenites*

535 (Fauquette et al., 2006) is present. This could be driven by four possible factors: 1) taphonomy i.e., the

536 assemblage has a high proportion of autochthonous spores and pollen with little input from the peripheral

537 mountains, 2) elevation of this region was relatively low in the middle–late Eocene (< 3000m as proposed by

538 Botsyun et al., 2019; also see Wei et al., 2016), 3) due to the generally wetter climate in relation to the

539 northeastern plateau basins, conifers are not competitive and surrounding mountains are instead forested by

540 temperate angiosperms, and 4) central Tibet recorded regional pollen transported by different atmospheric

541 circulation systems.

542 Regarding the first possibility, conifers are windblown and can be transported far distances (Lu et al., 2008;

543 Ma et al., 2008; Zhou et al., 2011); as the region already likely experienced a monsoonal climate (Spicer, 2017;

544 Licht et al., 2014; Caves et al., 2017; this study) we consider it unlikely that our assemblages record little to no

545 regional vegetation. The second factor, elevation history of the TP, is a controversial topic of discussion, and

546 palynological evidence from the RZ section does not provide strong support either for or against a relatively low

547 middle–late Eocene palaeoaltitude in the region. Although the upper part of the RZ section in the Nangqian

548 Basin likely just pre-dates the high-elevation signal further to the north from 37 Ma onwards (Dupont-Nivet et

549 al., 2008; Hoorn et al., 2012; Page et al., 2019), an expanding body of data indicates that a proto-Tibetan

550 Highland with complex topography was already in place during the Paleogene (Xu et al., 2013; Ding et al.,

551 2014; Wang et al., 2014; Valdes et al., 2019).

552   Isotopic evidence suggests moderate to high elevations for the Nangqian Basin in the late Eocene (valley

553   floor 2.7 (+0.6/–0.4) km above sea level; surrounding mountains 3.0 ± 1.1 km above sea level; Li L. et al.,

554   2019). In the adjacent Gonjo Basin, stable isotope data suggest the basin had already attained 2100–2500 m

555   palaeoelevation by the early Eocene (Tang et al., 2017). Some of the broad-leaved angiosperms trees present in

556   the new Nangqian assemblage could have grown at maximum elevations of 3600–4000 m during the Eocene

557   (*Ilex, Quercus*: Song et al., 2010), and therefore their presence in lieu of abundant conifers is not in

558   contradiction with an elevated topography in parts of east-central Tibet at this time. This has significance for

559   other Asian palynological studies that infer regional palaeoaltitudes and uplift history of Tibet based solely on

560   palynological records from a single locality: a multi-proxy approach is clearly necessary to address the complex

561   history of Tibetan uplift in future research.

562   Palynological data from the RZ assemblage supports climate (the third possibility) rather than altitude as a

563   primary driving factor of vegetational composition: locally wetter conditions in the east-central region of the TP

564   (see Section 5.2) would likely have promoted angiosperm tree growth over cold-temperate conifers that can

565   withstand drought better, and utilise a winter wet growing season unlike deciduous angiosperms (Dupont-Nivet

566   et al., 2008; Hoorn et al., 2012; Page et al., 2019). The last possibility is also supported, with the palynology of

567   this study suggesting that central Tibet was influenced by two atmospheric circulation systems: predominantly

568   the westerlies from the north (Caves Rugenstein and Chamberlain, 2018), and (to a limited degree) by a

569   southern monsoon, which could conceivably also have transported wind-blown pollen from sub-tropical and

570   warm temperate broad-leaved forests in the south (Su et al., 2018). Today, the Nangqian region receives nearly

571   70% of its moisture from the SAM, with the Westerlies from the north making up the remainder (Li L. et al.,

572   2019). This indicates that atmospheric circulation systems have changed considerably in east-central Tibet from

573   the Paleogene to Neogene, despite the existence of monsoons in this region since at least the Eocene (Licht et

574   al., 2014; Caves et al., 2017; Spicer, 2017). Based on the above, we propose that both local climatic conditions

575   and the influence of different regional atmospheric circulation systems contributed to the development of a

576   unique floral ecosystem in east-central Tibet during the late Eocene.

577

578   **6.   Conclusions**

579   On the basis of palynological assemblages, we conclude that the rocks of the RZ section (Nangqian Basin)

580   are Bartonian (41.2–37.8 Ma; late Eocene) in age. They record a strongly seasonal steppe-desert ecosystem

581 characterised by *Ephedra* and *Nitraria* shrubs, diverse ferns and an underlying component of broad-leaved

582 forests. The climate became significantly warmer for a short period, encouraging regional forest growth and a

583 proliferation of the thermophilic ancestral *Ephedra* type, but rapidly aridified thereafter due primarily to

584 regression of the proto-Paratethys Sea. This is in conjunction with observed environmental shifts in northeastern

585 Tibet, suggesting widespread Asian aridification in the late Eocene. A new palynozonation better constrains the

586 biostratigraphy of Paleogene successions across the northern, central, and southern TP, and also illustrates local

587 ecological variability during the Eocene. This highlights the ongoing challenge of integrating various deep time

588 records for the purpose of reconstructing palaeoelevation, and suggests that a multiproxy approach is vital for

589 unravelling the complex uplift history of the Qinghai-Tibetan region.

590

591 **Author contribution**

592 Q.Y., V.V., F.S.S., D.L.G., H.C.W. and Q.S.F. conceptualized the study. Q.Y., F.S.S., H.C.W., Z.J.Q., Y.S.D.

593 and J.J.S. carried out fieldwork. Q.Y., N.B., V.V. and C.R. collected and analysed the data. Q.Y. wrote the first

594 draft and N.B., V.V., and C.R. participated in review and editing of the final draft.

595

596 **Competing interests**

597 The authors declare that they have no conflict of interest.

598

610

611 **Data availability**

612   The authors declare that all data supporting the findings of this study are available in the supplementary

613 information or published in a data repository at the following DOI: http://dx.doi.org/10.17632/xvp68wsd2p.4.

614

615 **Supplementary information**

616   Supplementary information is available for this paper (Fig. S1, S2).

617

618 **References**

619 Abels, H. A., Dupont‑Nivet, G., Xiao, G., Bosboom, R., and Krijgsman, W.: Step‑wise change of Asian

620   interior climate preceding the Eocene‑Oligocene Transition (EOT), Palaeogeogr. Palaeoclimatol.

621   Palaeoecol., 299, 399–412, 2011.

622 Aitchison, J.C., and Davis, A.M.: When did the India–Asia collision really happen? Gondwana. Res., 4, 560–

623   561, 2001.

624 Aitchison, J.C., Xia, X.P., Baxter, A.T., and Ali, J.R.: Detrital zircon U-Pb ages along the Yarlung-Tsangpo

625   suture zone, Tibet: implications for oblique convergence and collision between India and Asia, Gondwana.

626   Res., 20, 691–709, 2011.

627 Baumann, F., He, J.S., Scheidt, K., Kühn, P., and Scholten, T.: Pedogenesis, permafrost, and soil moisture as

628   controlling factors for soil nitrogen and carbon contents across the Tibetan Plateau, Glob. Change Biol., 15,

629   3001–3017, 2009.

630 Bolinder, K., Norbäck Ivarsson, L., Humphreys, A.M., Ickert-Bond, S.M., Han, F., Hoorn, C., and Rydin, C.:

631   Pollen morphology of *Ephedra* (Gnetales) and its evolutionary implications, Grana, 55, 24–51, 2016.

632 Bosboom, R.E., Dupont-Nivet, G., Houben, A.J.P., Brinkhuis, H., Villa, G., Mandic, O., Stoica, M., Zachariasse,

633   W.J., Guo, Z.J, Li, C.X, and Krijgsman, W.: Late Eocene sea retreat from the Tarim Basin (west China) and

634   concomitant Asian paleoenvironmental change, Palaeogeogr. Palaeoclimatol. Palaeoecol., 299, 385–398,

635   2011.

636 Bosboom, R.E., Abels, H.A., Hoorn, G., Van den berg, B.C.J., Guo, Z.J., and Dupont-Nivet, G.: Aridification in

637   continental Asia after the Middle Eocene Climatic Optimum (MECO), Earth Planet. Sci. Lett., 389, 34–42,

638   2014.

639 Botsyun, S., Sepulchre, P., Donnadieu, Y., Risi, C., Licht, A., and Caves Rugenstein, J.: Revised paleoaltimetry

640   data show low Tibetan Plateau elevation during the Eocene, Science, 363, eaaq1436, 2019.

641   Bougeois, L., Dupont-Nivet, G., De Rafélis, M., Tindall, J., Proust, J.N., Reichart, G.J., Nooijer, L., Guo, Z.J.,

642   and Ormukov, C.: Asian monsoons and aridification response to Paleogene sea retreat and Neogene

643   westerly shielding indicated by seasonality in Paratethys oysters, Earth Planet. Sci. Lett., 485, 99–110,

644   2018.

645   Cai, M.T., Fang, X.M., Wu, F.L., Miao, Y.F., and Appel, E.: Pliocene–Pleistocene stepwise drying of Central

646   Asia: evidence from paleo-magnetism and sporopollen record of the deep borehole SG-3 in the western

647   Qaidam Basin, NE Tibetan Plateau, Global. Planet. Change, 94–95, 72–81, 2012.Caves, J.K., Sjostrom,

648   D.J., Mix, H.T., Winnick, M.J., and Chamberlain, C.P.: Aridification of Central Asia and uplift of the Altai

649   and Hangay Mountains, Mongolia: Stable isotope evidence, Am. J. Sci., 314. 1171–1201, 2014.

650   Caves, J.K., Winnick, M.J., Graham, S.A., Sjostrom, D.J., Mulch, A., and Chamberlain, C.P.: Role of the

651   westerlies in Central Asia climate over the Cenozoic, Earth Planet. Sci. Lett., 428, 33–43, 2015.

652   Caves, J.K., Moragne, D.Y., Ibarra, D.E., Bayshashov, B.U., Gao, Y., Jones, M.M., Zhamangara, A.,

653   Arzhannikova, A.V., Arzhannikov, S.G. and Chamberlain, C.P.: The Neogene de-greening of Central Asia.

654   Geology, 44(11), 887–890, 2016.

655   Caves Rugenstein, J.K. and Chamberlain, C.P.: The evolution of hydroclimate in Asia over the Cenozoic: A

656   stable-isotope perspective. Earth-Science Reviews, 185, 1129–1156, 2018.

657   Cour, P., Zheng, Z., Duzer, D., Calleja, M., and Yao, Z.: Vegetational and climatic significance of modern pollen

658   rain in northwestern Tibet, Rev. Palaeobot. Palynol., 104, 183–204, 1999.

659   DeConto, R.M., and Pollard, D.: Rapid Cenozoic glaciation of Antarctica induced by declining atmospheric

660   CO_2, Nature, 421, 245–249, 2003.

661   Deng, W., Sun, H., and Zhang, Y.: Cenozoic K–Ar ages of volcanic rocks in the Nangqian Basin, Qinghai,

662   Chinese Sci. Bull., 44, 2554–2558, 1999. (in Chinese with English abstract).

663   Ding, L., Xu, Q., Yue, Y.H., Wang, H.Q., Cai, F.I., and Li, S.: The Andean-type Gangdese Mountains:

664   paleoelevation record from the Paleocene-Eocene Linzhou Basin, Earth Planet. Sci. Lett., 392, 250–264,

665   2014.

666   Du, H F., Jiang Y B., Yan Z B., Hou Z Q., Yang T N., Guo F S., and Yang Q K.: Sedimentary Characteristics and

667   Environment of the Paleogene Nangqian Basin in Qinghai Province. Acta Geologica Sinica 85(3), 383–

668   395, 2011. (in Chinese with English abstract).

669   Dupont-Nivet, G., Keijgsman, W., Langereis, C.G., Abels, H.A., Dai, S., and Fang, X.M.: Tibetan plateau

670   aridification linked to global cooling at the Eocene-Oligocene transition, Nature, 445, 635-638, 2007.

671 Dupont-Nivet, G., Hoorn, C., and Konert, M.: Tibetan uplift prior to the Eocene–Oligocene climate transition:

672   evidence from pollen analysis of the Xining Basin, Geology, 36, 987–990, 2008.

673 Fauquette, S., Suc, J.P., Bertini, A., Popescu, S.M., Warny, S., Taoufiq, N.B., Villa, M.J.P., Chikhi, H., Feddi, N.,

674   Subally, D., and Clauzon, G.: How much did climate force the Messinian salinity crisis? Quantified

675   climatic conditions from pollen records in the Mediterranean region, Palaeogeogr. Palaeoclimatol.

676   Palaeoecol., 238, 281–301, 2006.

677 Grimm, E.C.: CONISS: a FORTRAN 77 program for stratigraphically constrained cluster analysis by the

678   method of incremental sum of squares. Comput Geosci UK., 13(1), 13–35, 1987.

679 Grimm, E.C.: TILIA v2. 0. b. 4 and TGView v2. 0 (computer software), Illinois State Museum, Research and

680   Collections Center, Springfield, IL, USA, 1991. https://www.tiliait.com/

681 Gupta, A. K., Singh, R. K., Joseph, S., and Thomas, E.: Indian Ocean high-productivity event (10–8 Ma):

682   Linked to global cooling or to the initiation of the Indian monsoons? Geology, 32, 753–756, 2004.

683 Han, F., Rydin, C., Bolinder, K., Dupont-Nivet, G., Abels, H.A., Koutsodendris, A., Zhang, K., and Hoorn, C.:

684   Steppe development on the Northern Tibetan Plateau inferred from Paleogene ephedroid pollen, Grana, 55,

685   71–100, 2016.

686 Han, J.L., Han, F.Q., Hussain, S.A., Liu, W.Y., Nian, X.Q., and Mao, Q.F.: Origin of Boron and Brine Evolution

687   in Saline Springs in the Nangqen Basin, Southern Tibetan Plateau, Geofluids, 2018, 1–12, 2018.

688 Herb, C., Koutsodendris, A., Zhang, W.L., Appel, E., Fang, X.M., Voigt, S., and Pross, J.: Late Plio-Pleistocene

689   humidity fluctuations in the western Qaidam Basin (NE Tibetan Plateau) revealed by an integrated

690   magnetic-palynological record from lacustrine sediments, Quat. Res., 84, 457–466, 2015.

691 Herzschuh, U., Tarasov, P., Wünnemann, B., and Hartmann, K., Holocene vegetation and climate of the Alashan

692   Plateau NW China, reconstructed from pollen data, Palaeogeogr. Palaeoclimatol. Palaeoecol., 211, 1–17,

693   2004.

694 Herzschuh, U., and Liu, X.Q.: Vegetation evolution in arid China during Marine Isotope Stages 3 and 2 (~ 65–

695 11 Ka). Developments in Quaternary, Science, 9, 41–49, 2007.

696 Hoorn, C., Straathof, J., Abels, H.A., Xu, Y.D., Utescher, T., and Dupont-Nivet, G.: A late Eocene palynological

697   record of climate change and the Tibetan Plateau uplift (Xining Basin, China), Palaeogeogr. Palaeoclimatol.

698   Palaeoecol., 344, 16–38, 2012.

699 Horton, B.K., Yin, A., Spurlin, M.S., Zhou, J., and Wang, J.: Paleocene–Eocene syncontractional sedimentation

700   I n narrow, lacustrine-dominated basins of east-central Tibet, Geol. Soc. Ame. Bull., 114, 771–786, 2002.

701   Hou, Z., Hongwen, M., Zaw, K., Yuquan, Z., Mingjie, W., Zeng, W., Guitang, P., and Renli, T.: The Himalayan

702   Yulong porphyry copper belt: product of large-scale strike-slip faulting in eastern Tibet, Econ. Geol., 98,

703   125–145, 2003.

704   Hu, X.M., Garzanti, E., Wang, J.G., Huang, W.T., An, W., and Webb, A.: The timing of India-Asia collision

705   onset- Facts, theories, controversies, Earth-Sci. Rev., 160, 264–299, 2016.

706   Ji, L.M., Meng, F.W., Yan, K., and Song, Z.G.: The dinoflagellate cyst Sub-tilisphaera from the Eocene of the

707   Qaidam Basin, northwest China, and its implications for hydrocarbon exploration, Rev. Palaeobot.

708   Palynol., 167, 40–50, 2011.

709   Jiang, H., and Ding, Z.: A 20 Ma pollen record of East-Asian summer monsoon evolution from Guyuan, Nigxia,

710   China, Palaeogeogr. Palaeoclimatol. Palaeoecol., 265, 30–38, 2008.

711   Jiang, Y.B., Guo, F.S., Hou, Z.Q., Yang, T.N., Liu, Y.X., Yang, Q.K., and Du, H.F.: Sedimentary features and

712   evolution of the Nangqian Paleogene basin in northeastern Qinghai-Tibet Plateau, Acta petrol. Et. Miner.,

713   30, 391–400, 2011. (in Chinese with English abstract).

714   Jin, C., Liu, Q., Liang, W., Roberts, A.P., Sun, J., Hu, P., Zhao, X., Su, Y., Jiang, Z., Liu, Z. and Duan, Z.:

715   Magnetostratigraphy of the Fenghuoshan Group in the Hoh Xil Basin and its tectonic implications for

716   India–Eurasia collision and Tibetan Plateau deformation, Earth Planet. Sci. Lett., 486, 41–53, 2018.

717   Kaya, M.Y., Dupont-Nivet, G., Proust, J-N., Roperch, P., Bougeois, L., Meijer, N., Frieling, J., Fioroni, C.,

718   Altiner, S.Ö., Vardar, E., Barbolini, N., Stoica, M., Aminov, J., Mamtimin, M., and Guo, Z.: Paleogene

719   evolution and demise of the proto-Paratethys Sea in Central Asia (Tarim and Tajik basins): role of

720   intensified tectonic activity at ~41 Ma, Basin Res., 31, 461–486, 2019.

721   Kotthoff, U., Greenwood, D.R., McCarthy, F.M.G., Müller-Navarra, K., Prader, S., and Hesselbo, S.P.: Late

722   Eocene to middle Miocene (33 to 13 million years ago) vegetation and climate development on the North

723   American Atlantic Coastal Plain (IODP Expedition 313, Site M0027), Clim. Past., 10, 1523–1539, 2014.

724   Li, F., Sun, J., Zhao, Y., Guo, X., Zhao, W. and Zhang, K.: Ecological significance of common pollen ratios: A

725   review. Front, Earth Sci. Chin., 4(3), 253–258, 2010.

726   Li, J.F., Xie, G., Yang, J., Ferguson, D.K., Liu, X.D., Liu, H. and Wang, Y.F.: Asian Summer Monsoon changes

727   the pollen flow on the Tibetan Plateau. Earth-Science Reviews, 202, 103–114, 2020.

728   Li, J.G., Batten, D.J., and Zhang, Y.Y.: Palynological indications of environmental changes during the Late

729   Cretaceous–Eocene on the southern continental margin of Laurasia, Xizang (Tibet), Palaeogeogr.

730   Palaeoclimatol. Palaeoecol., 265, 78–86, 2008.

731   Li, J.G., Wu, Y.X., Batten, D.J., and Lin, M.Q.: Vegetation and climate of the central and northern Qinghai–

732   Xizang plateau from the Middle Jurassic to the end of the Paleogene inferred from palynology, J. Asian.

733   Earth. Sci., 175, 34–38, 2019.

734   Li, L., Fan, M., Davila, N., Jesmok, G., Mitsunaga, B., Tripati, A. and Orme, D.: Carbonate stable and clumped

735   isotopic evidence for late Eocene moderate to high elevation of the east-central Tibetan Plateau and its

736   geodynamic implications. Bulletin, 131(5-6), 831–844, 2019.

737   Li, S.Y., Currie, B.S., Rowley, D.B., and Ingalls, M.: Cenozoic paleoaltimetry of the SE margin of the Tibetan

738   Plateau: Constraints on the tectonic evolution of the region, Earth Planet. Sci. Lett., 432, 415-424, 2015.

739   Li, Y., Xu, Q., Zhao, Y., Yang, X., Xiao, J., Chen, H., and Lü, X.: Pollen indication to source plants in the

740   eastern desert of China, Chinese. Sci. Bull., 50 (15), 1632–1641, 2005.

741   Li, Y., Wang, N., Morrill, C., Cheng, H., Long, H., and Zhao, Q.: Environmental change implied by the

742   relationship between pollen assemblages and grain-size in N.W. Chinese lake sediments since the Late

743   Glacial, Rev. Palaeobot. Palynol., 154, 54–64, 2009.

744   Li, X., Zhang, R., Zhang, Z. and Yan, Q.: What enhanced the aridity in Eocene Asian inland: Global cooling or

745   early Tibetan Plateau uplift? Palaeogeogr. Palaeoclimatol. Palaeoecol., 510, 6–14, 2018.

746   Licht, A., Cappelle, M.V., Ables, H.A., Ladant, J.B., Trabucho-Alexandre, J., France-Lanord, C., Donnadieu, Y.,

747   Vandenberghe, J., Rigaudier, T., Lecuyer, C., Terry Jr, D., Adriaens, R., Boura, A., Guo, Z., Soe, A.N.,

748   Quade, J., Dupont-Nivet, G., Jaeger, J.J.: Asian monsoons in a late Eocene greenhouse world, Nature,

749   513, 501–506, 2014.

750   Linnemann, U., Su, T., Kunzmann, L., Spicer, R.A., Ding, W.N., Spicer, T.E.V., Zieger, J., Hofmann, M.,

751   Moraweck, K., Gärtner, A. and Gerdes, A.: New U-Pb dates show a Paleogene origin for the modern

752   Asian biodiversity hot spots. Geology, 46(1), 3–6, 2018.

753   Liu, G.W., *Fupingopollenites* gen. nov. and its distribution, Acta. Palaeontol. Sin., 24, 64–70, 1985. (in Chinese

754   with English abstract).

755   Liu, J., Li, J.J., Song, C.H., Yu, H., Peng, T.J., Hui, Z.C., and Ye, X.Y.: Palynological evidence for late Miocene

756   stepwise aridification on the northeastern Tibetan Plateau, Clim. Past, 12, 1473–1484, 2016.

757   Liu, Y., Liu, H., Theye, T. and Massonne, H.J.: Evidence for oceanic subduction at the NE Gondwana margin

758   during Permo-Triassic times, Terra Nova, 21(3), 195–202, 2009.

759   Liu, Z., Zhao, X., Wang, C.S., and Liu, H.Y.: Magnetostratigraphy of Tertiary sediments from the Hoh Xil

760   Basin: implications for the Cenozoic tectonic history of the Tibetan Plateau, J. Asian. Earth. Sci., 154,

761   233–252, 2003.

762 Liu, Z.Q.: Geologic map of the Qinghai-Xizang Plateau and its neighboring regions: Beijing, Chengdu Institute

763   of Geology and Mineral Resources, Geologic Publishing House, scale 1:1 500 000. 1988.

764 Lu, H., Wu, N., Yang, X., Shen, C., Zhu, L., Wang, L., Li, Q., Xu, D., Tong, G., and Sun, X.: Spatial patterns of

765   Abies and Picea surface pollen distribution along the elevation gradient in the Qinghai–Tibetan Plateau and

766   Xinjiang, China, Boreas, 37, 254–262, 2008.

767 Lu, J.F., Song, B.W., Chen, R.M., Zhang, J.Y., and Ye, H.: Palynological assemblage of Eocene–Oligocene

768   pollen and their biostratigraphic correlation in Dahonggou, Daqaidam Regions, Qaidam Basin, Earth Sci. J.

769   China University of Geosciences, 35, 839–848, 2010. (in Chinese, with English abstract).

770 Ma, Y., Liu, K., Feng, Z., Sang, Y., Wang, W., and Sun, A.: A survey of modern pollen and vegetation along a

771   south–north transect in Mongolia, J. Biogeogr., 35, 1512–1532, 2008.

772 Mao, Y.B.: Tectonic evolvement Coal accumulation in Zaduo-Nangqian area of Qinghai Province, J. Earth Sci.

773   Environ., 32, 225–233, 2010. (in Chinese)

774 Meijer, N., Dupont-Nivet, G., Abels, H.A., Kaya, M.Y., Licht, A., Xiao, M.M., Zhang, Y., Roperch, P., Poujol,

775   M., Lai, Z.P., and Guo, Z.J.: Central Asian moisture modulated by proto-Parathethys Sea incursions since the

776   early Eocene, Earth Planet. Sci. Lett., 510. 73–84, 2019.

777 Miao, Y.F.: Cenozoic Pollen Records in the Xining Basin and Its Significance for the Palaeoclimate Change.

778   Postdoctoral Report. Institute of Tibetan Plateau Research, Chinese Academy of Sciences, Beijing, 95 pp,

779   2010. (in Chinese with English abstract).

780 Miao, Y.F., Fang, X.M., Song, Z.C., Wu, F.L., Han, W.X., Dai, S. and Song, C.H.: Late Eocene pollen records

781   and paleoenvironmental changes in northern Tibetan Plateau, Sci. China. Earth. Sci., 51, 1089–1098, 2008.

782 Miao, Y.F., Fang, X.M., Herrmann, M., Wu, F.L., Zhang, Y.Z., and Liu, D.L.: Miocene pollen record of KC-1

783   core in the Qaidam Basin, NE Tibetan Plateau and implications for evolution of the East Asian monsoon,

784   Palaeogeogr. Palaeoclimatol. Palaeoecol., 299, 30–38, 2011.

785 Miao, Y.F., Herrmann, M., Wu, F.L., Yan, X.L., and Yang, S.L.: What controlled Mid-Late Miocene long-term

786   aridification in Central Asia? Global cooling or Tibetan Plateau uplift: a review, Earth. Sci. Rev., 112, 155–

787   172, 2012.

788 Miao, Y.F., Fang, X.M., Wu, F.L., and Cai, M.T.: Late Cenozoic continuous aridification in the western Qaidam

789   Basin: evidence from sporopollen records, Clim. Past. 9, 1863–1877, 2013a.

790 Miao, Y.F., Fang, X.M., Song, C.H., Yan, X.L., Xu, L., and Chen, C.F.: Pollen and fossil wood's linkage with

791   Mi-1 Glaciation in northeastern Tibetan Plateau, China, Palaeoworld, 22, 101–108, 2013b.

792 Miao, Y.F., Wu, F.L., Chang, H., Fang, X.M., Deng, T., Sun, X.M., and Jin, C.S.: A Late Eocene palynological

793   record from the Hoh Xil Basin, Northern Tibetan Plateau, and its implications for stratigraphic age,

794   paleoclimate and paleoelevation, Gondwana. Res., 31, 241–252, 2016.

795 Molnar, P.: Late Cenozoic increase in accumulation rates of terrestrial sediments: How might climate change

796   have affected erosion rates? Annu. Rev. Earth Planet. Sci., 32, 67–89, 2004.

797 Molnar, P., and Tapponnier, P.: Effects of a Continental Collision, Science, 189, 419–426, 1975.

798 Molnar, P., Boos, W.R., and Battisti, D.S.: Orographic controls on climate and paleoclimate of Asia: thermal and

799   mechanical roles for the Tibetan Plateau, Annu. Rev. Earth Planet. Sci., 38, 77–102, 2010.

800 Mulch, A., and Chamberlain, C.P.: Stable isotope paleoaltimetry in orogenic belts — the silicate record in

801   surface and crustal geological archives, Reviews in Mineralogy and Geochemistry, 66, 89–118, 2007.

802 Paeth, H., Steger, C., Li, J.M., Mutz, S.G. and Ehlers, T.A.: Comparison of Cenozoic surface uplift and glacial-

803   interglacial cycles on Himalaya-Tibet paleo-climate: Insights from a regional climate model, Global

804   Planet. Change, 177, 10–26, 2019.

805 Page, M., Licht, A., and Dupont-Nivet, G.: Synchronous cooling and decline in monsoonal rainfall in

806   northeastern Tibet during the fall into the Oligocene icehouse, Geology, 47(3), 203–206, 2019.

807 Pagani, M., Hubei, M., Liu, Z.H., Bohaty, S.M., Henderikes, J., Sijp, W., Krishnan, S., and DeConto, R.M.: The

808   role of carbon dioxide during the onset of Antarctic glaciation, Science, 334, 1261–1264, 2011.

809 Qinghai BGMR, (Qinghai Bureau of Geology and Mineral Resources), Geologic map of the Nangqian region,

810   with geologic report: unpublished, 198 pp., scale 1:200 000. 1983a.

811 Qinghai BGMR, (Qinghai Bureau of Geology and Mineral Resources), Geologic map of the Shanglaxiu region,

812   with geologic report: unpublished, 220 pp., scale 1:200 000. 1983b.

813 Qinghai BGMR, (Qinghai Bureau of Geology and Mineral Resources), Regional Geology of Qinghai Province:

814   Beijing, Geological Publishing House, 662 pp. 1991.

815 Rowley, D.B., and Currie, B.S.: Palaeo-altimetry of the late Eocene to Miocene Lunpola basin, central Tibet,

816   Nature, 439, 677–681, 2006.

817 Shen, H., and Poulsen, C.J.: Precipitation δ18O on the Himalaya–Tibet orogeny and its relationship to surface

818   elevation, Clim. Past, 15, 169–187, 2019.

819 Song, X.Y., Spicer, R.A., Yan, J., Yao, Y.F., and Li, C.S.: Pollen evidence for an Eocene to Miocene elevation of

820   central southern Tibet predating the rise of the High Himalaya, Palaeogeogr. Palaeoclimatol. Palaeoecol.,

821   297, 159–168, 2010.

822 Song, Z.C., and Liu, G.W.: Early Tertiary palynoflora and its significance of palaeogeography from northern and

823   eastern Xizang. In: Integrative Scientific Expedition Team to the Qinghai–Xizang plateau, Academia

824   Sinica (ed.), Palaeontology of Xizang. Book V. Science Press, Beijing, 183–201, 1982. (in Chinese with

825   English abstract).Spicer, R.A.: Tibet, the Himalaya, Asian monsoons and biodiversity in what ways are

826   they related? Plant Diversity, 39, 233–244, 2017.

827 Spicer, R.A., Su, T., Valdes, P.J., Farnsworth, A., Wu, F.X., Shi, G., Spicer, T.E. and Zhou, Z.: Why the 'Uplift of

828   the Tibetan Plateau' is a myth. National Science Review, nwaa091, https://doi.org/10.1093/nsr/nwaa091,

829   2020.

830 Spurlin, M.S., Yin, A., Horton, B.K., Zhou, J., and Wang, J.: Structural evolution of the Yushu–Nangqian region

831   and its relationship to syncollisional igneous activity, east-central Tibet, Geol. Soc. Am. Bull., 117, 1293–

832   1317, 2005.

833 Stanley, C., Charlet, D.A., Freitag, H., Maier-Stolte, M., and Starratt, A.N.: New observations on the secondary

834   chemistry of world *Ephedra* (Ephedraceae), Am. J. Bot., 88, 1199–1208, 2001.

835 Studnicki-Gizbert, C., Burchfiel, B.C., Li, Z. and Chen, Z.: Early Tertiary Gonjo basin, eastern Tibet:

836   Sedimentary and structural record of the early history of India-Asia collision. Geosphere, 4(4), 713–735,

837   2008.

838 Su, T., Spicer, R.A., Li, S.H., Huang, J., Sherlock, S., Huang, Y.J., Li, S.F., Wang, Li., Jia, L.B., Deng, W.Y.D.,

839   Liu, J., Deng, C.L., Zhang, S.T., Valdes, P.J., and Zhou, Z.K.: Uplift, climate and biotic changes at the

840   Eocene-Oligocene transition in south-eastern Tibet, Natl. Sci. Rev., 6(3), 495–504, 2018.

841 Su, T., Farnsworth, A., Spicer, R.A., Huang, J., Wu, F.X., Liu, J., Li, S.F., Xing, Y.W., Huang, Y.J., Deng,

842   W.Y.D., Tang, H., Xu, C.L., Zhao, F., Srivastava, G., Valdes, P.J., Deng, T., and Zhou, Z.K.: No high

843   Tibetan Plateau until the Neogene, Science Advances, 5, 1–8, 2019.

844 Sun, X.J., and Wang, P.X.: How old is the Asian monsoon system—palaeobotanical records from China,

845   Palaeogeogr. Palaeoclimatol. Palaeoecol., 222, 181–222, 2005.

846 Sun, Z., Yang, Z.Y., Pei, X.H., Wang, X.S., Yang, T.S., Li, W.M., and Yuan, S.H.: Magnetostratigraphy of

847   Paleogene sediments from northern Qaidam Basin, China: implications for tectonic uplift and block

848   rotation in northern Tibetan plateau, Earth Planet. Sci. Lett., 237, 635–646, 2005.

849 Sun, Z.C., Feng, X.J., Li, D.M., Yang, F., Qu, Y.H., and Wang, H.J.: Cenozoic Ostracoda and

850   palaeoenvironments of the northeastern Tarim Basin western China, Palaeogeogr. Palaeoclimatol.

851   Palaeoecol.148, 37–50, 1999.

852   Tang, M., Liu-Zeng, J., Hoke, G.D., Xu, Q., Wang, W., Li, Z., Zhang, J. and Wang, W.: Paleoelevation

853   reconstruction of the Paleocene-Eocene Gonjo basin, SE-central Tibet. Tectonophysics, 712, 170–181,

854   2017.

855   Tarasov, P.E., Cheddadi, R., Guiot, J., Bottema, S., Peyron, O., Belmonte, J., Ruiz-sanchez, V., Saadi, F., and

856   Brewer, S.: A method to determine warm and cool steppe biomes from pollen data; application to the

857   Mediterranean and Kazakhstan regions, J. Quat. Sci., 13, 335–344, 1998.

858   Tardif, D., Fluteau, F., Donnadieu, Y., Le Hir, G., Ladant, J.B., Sepulchre, P., Licht, A., Poblete, F. and Dupont-

859   Nivet, G.: The origin of Asian monsoons: a modelling perspective. Climate of the Past, 16(3), 847–865,

860   2020.

861   Valdes, P.J., Lin, D., Farnsworth, A., Spicer, R.A., Li, S.H. and Tao, S.: Comment on "Revised paleoaltimetry

862   data show low Tibetan Plateau elevation during the Eocene", Science, 365(6459), eaax8474, 2019.

863   Wang, C.S., Zhao, X.X., Liu, Z.Z., Peter, C., Stephan, A.G., Robert, S.C., Zhu, L.D., Liu, S., and Li, Y.L.:

864   Constraints on the early uplift history of the Tibetan Plateau, Proc. Natl. Acad. Sci. USA., 105, 4987–4992,

865   2008.

866   Wang C.S., Dai, J.G., Zhao, X.X., Li, Y.L., Graham, S.A., He, D.F., Ran, B., and Meng, J.: Outward-growth of

867   the Tibetan Plateau during the Cenozoic: A review, Tectonophysics, 621, 1–43, 2014.

868   Wang, C.W., Hong, H.L., Li, Z.H., Yin, K., Xie, J., Liang, G.J., Song, B., Song, E., Zhang, K.X.: The Eocene–

869   Oligocene climate transition in the Tarim Basin, Northwest China: evidence from clay mineralogy, Appl.

870   Clay. Sci., 74, 10–19, 2013.

871   Wang, D., Sun, X.Y., and Zhao, Y.: Late Cretaceous to Tertiary palynofloras in Xingjiang and Qinghai China,

872   Rev. Palaeobot. Palynol., 65, 95–104, 1990a.

873   Wang, D., Sun, X.Y., Zhao, Y., He, Z.: Palynoflora from Late Cretaceous to Tertiary in Some Regions of

874   Qinghai and Xinjiang, China Environmental Science Press, Beijing, pp. 1–179, 1990b. (in Chinese with

875   English abstract).

876   Wang, J., Wang, Y.J., Liu, Z.C., Li, J.Q., and Xi, P.: Cenozoic environmental evolution of the Qaidam Basin and

877   its implications for the uplift of the Tibetan Plateau and the drying of central Asia, Palaeogeogr.

878   Palaeoclimatol. Palaeoecol., 152, 37–47, 1999.

879   Wang, S.F., Yi, H.S., and Wang, C.S.: Sedimentary facies and palaeogeography features of Nangqian Tertiary

880   basin in Yushu district, Qinghai, Northwestern Geol., 34, 64–67, 2001. (in Chinese, with English abstract).

881 Wang, S.F., Yi, H.S., and Wang, C.S.: Sediments and structural features of Nangqian Tertiary Basin in eastern of

882   Tibet-Qingzang Plateau, Acta Sci. Nat. Univ. Pekin., 38, 109–114, 2002. (in Chinese, with English

883   abstract).

884 Wang Z.: A new Permian gnetalean cone as fossil evidence for supporting current molecular phylogeny, Ann.

885   Bot., 94, 281–288, 2004.

886 Wang, Z.X., Shen, Y.J., and Pang, Z.B.: Three main stages in the uplift of the Tibetan Plateau during the

887   Cenozoic period and its possible effects on Asian aridification: A review, Clim. Past Discuss,

888   https://doi.org/10.5194/cp-2018-64, 2018.

889 Wei, H.C., Fan, Q.S., Zhao, Y., Ma, H.Z., Shan, F.S., An, F.Y., and Yuan, Q.: A 94-10 Ka pollen record of

890   vegetation change in Qaidam Basin, northeastern Tibetan Plateau, Palaeogeogr. Palaeoclimatol.

891   Palaeoecol., 431, 43–52, 2015.

892 Wei, M.: Eogene ostracods from Nangqen in Qinghai. Contribution to the Geology of the Qinghai-Xizang

893   (Tibet) Plateau, 17, 313–324, 1985. (in Chinese with English abstract). Geological Publishing House,

894   Beijing

895 Wei, Y., Zhang, K., Garzione, C.N., Xu, Y.D., Song, B., Ji, J.L.: Low palaeoelevation of the northern Lhasa

896   terrane during late Eocene: Fossil foraminifera and stable isotope evidence from the Gerze Basin, Sci.

897   Rep., 6, 27508, 2016.

898 Wu, J., Zhang, K., Xu, Y., Wang, G., Garzione, C.N., Eiler, J., Leloup, P.H., Sorrel, P. and Mahéo, G.:

899   Paleoelevations in the Jianchuan Basin of the southeastern Tibetan Plateau based on stable isotope and

900   pollen grain analyses. Palaeogeography, Palaeoclimatology, Palaeoecology, 510, 93–108, 2018.

901 Xia, L.Q., Li, X.G., Ma, Z.P., Xu, X.Y., and Xia, Z.C.: Cenozoic volcanism and tectonic evolution of the Tibetan

902   plateau, Gondwana. Res., 19, 850–866, 2011.

903 Xiao, G.Q., Abels, H.A., Yao, Z.Q., Dupont-Nivet, G., and Hilgen, F.J.: Asian aridification linked to the first

904   step of the Eocene-Oligocene climate Transition (EOT) in obliquity-dominated terrestrial records (Xining

905   Basin, China), Clim. Past, 6, 501–513, 2010.

906 Xu, Q., Ding, L., Zhang, L.Y., Cai, F.L., Lai, Q.Z., Yang, D., and Zeng, J.L.: Paleogene high elevations in the

907   Qiangtang Terrane, central Tibetan Plateau, Earth Planet. Sci. Lett., 362, 31–42, 2013.

908 Xu, R., Song, Z.C., and Zhou, H.Y., The palynological assemblages in Tertiary sediments of Qaidam Basin and

909   its significance in geology, Acta. Palaeontol. Sin., 6, 429–440, 1958 (in Chinese).

910 Xu, Y., Bi, X.W., Hu, R.Z., Chen, Y.W., Liu, H.Q., and Xu, L.L.: Geochronology and geochemistry of Eocene

potassic felsic intrusions in the Nangqian basin, eastern Tibet: Tectonic and metallogenic implications, Lithos., 246–247, 212–227, 2016.

Yang, Y.: Systematic and Evolution of *Ephedra* L. (Ephedraceae) from China. PhD Thesis. Institute of Botany Chinese Academy of Sciences, Beijing, 231 pp. 2002. (in Chinese with English summary).

Yin, A., and Harrison, T.M.: Geologic evolution of the Himalayan–Tibetan orogeny, Annu. Rev. Earth. Pl. Sc., 28, 211–280, 2000.

Yuan, Q., Vajda, **V**., Li, Q.K., and Shan, F.S.: A late Eocene palynological record from the Nangqian Basin, Tibetan Plateau: Implications for stratigraphy and paleoclimate, Palaeoworld, 26: 369–379, 2017.

Yuan, Q., Barbolini, N., 2020. "Supplementary dataset: Aridification signatures from middle–late Eocene pollen indicate widespread drying across the Tibetan Plateau after 40 Ma". Mendeley Data. v4 http://dx.doi.org/10.17632/xvp68wsd2p.4

Yuan, Q., Barbolini, N., Ashworth, L., Rydin, C., Gao, D.L., Wei, H.C., Fan, Q.S., Qin, Z.J., Du, Y.S., Shan, J.J., Shan, F.S., and Vajda, V.: Palaeoenvironmental changes in Eocene Tibetan lake systems traced by geochemistry, sedimentology and palynofacies, ~~Terra Nova~~Journal of Asian Earth Sciences, submitted~~in prep~~.

Zachos, J., Pagani, M., Sloan, L., Thomas, E., and Billups, K.: Trends, rhythms, and aberrations in global climate 65 Ma to present, Science, 292, 686-693, 2001.

Zhang, J., Santosh, M., Wang, X., Guo, L., Yang, X., and Zhang, B.: Tectonics of the northern Himalaya since the India–Asia collision, Gondwana. Res., 21, 939–960, 2012.

Zhang, W.L.: The high precise Cenozoic magnetostratigraphy of the Qaidam Basin and uplift of the Northern Tibetan plateau, (PhD Thesis). Lanzhou University, Lanzhou, 109 pp, 2006.

Zhao, Y., Herzschuh, U.: Modern pollen representation of source vegetation in the Qaidam Basin and surrounding mountains, north-eastern Tibetan Plateau, Veg. Hist. Archaeobot., 18, 245–260, 2009.

Zhou, X.Y., and Li, X.Q.: Variations in spruce (*Picea* sp.) distribution in the Chinese Loess Plateau and surrounding areas during the Holocene, Holocene, 22, 687–696, 2011.

Zhu, H.C., Ouyang, S., Zhan, J.Z., and Wang, Z.: Comparison of Permian palynological assemblages from the Junggar and Tarim Basins and their phytoprovincial significance, Rev. Palaeobot. Palynol, 136, 181–207, 2005.

Zhu, L., Zhang, H.H., Wang, J.H., Zhou, J.Y., and Xie, G.H.: ^{40}Ar/^{39}Ar chronology of high-K magmatic rocks in Nangqian Basin at the northern segment of the Jinsha-Red River Shear Zone (JRRSZ), Geotecton. et

941   Metallog., 30, 241–247, 2006. (in Chinese, with English abstract).

942 Zhu, Z.H., Wu, L., Xi, P., Song, Z.C., and Zhang, Y.Y.: A Research on Tertiary Palynology from the Qaidam

943   Basin, Qinghai Province, Petroleum Industry Press, Beijing, 1–297, 1985. (in Chinese with English

944   abstract).